Speculative Dynamics and Currency Crash Risk

Makoto Nirei
Institute of Innovation Research
Hitotsubashi University

Vladyslav Sushko[‡]
University of California, Santa Cruz

November 5, 2010

Abstract

When domestic monetary policy considerations introduce an interest rate wedge between two countries, a trader can make a profit by borrowing at low interest in one country to fund the purchase of a higher yielding asset in the other. That is, unless the high yield currency depreciates sharply. We model strategic traders trying to profit from such interest rate differential at the expense of exposing themselves to currency crash risk. Because all such "carry traders" are concerned with the same type of foreign exchange risk they seek the same information and extract signals from each others' actions. In this environment, a random termination of a carry position can trigger a herd effect causing others to do the same. As the traders simultaneously pile on the low interest currency to repay their liabilities the fears of high yield currency crash become self-fulfilling. Such dynamics imply that sudden appreciations (depreciations) of low (high) yield currencies, although rare, are not independent events. This hypothesis is corroborated by the distribution of realized volatility jumps in the Japanese yen, which has served as a funding currency in carry trade. Yen *appreciation* jumps exhibit dependence and extreme variability, whereas *depreciation* jumps appear to be white noise. Consistent with our model predictions, we find that higher volume of carry trade positions increases the "tail risk" of sharp yen *appreciation* directly, while lower margin requirements and higher option implied risk premia only raise the likelihood of sharp *appreciation* indirectly through their effect via the actions of carry traders.

JEL Codes: C73, F31, G32

Keywords: Stochastic Games, Herd Behavior, Fat Tails, Foreign Exchange, Financial Risk and Risk Management

*Sushko is extremely grateful to Michael Hutchison for his guidance, data support, and for making this collaboration possible, to Takatoshi Ito for hosting him at the University of Tokyo where this collaboration began, and to Dan Friedman for his invaluable advice. We also thank Joshua Aizenman, Bertrand Candelon, Ai-Ru Cheng, Michael Dooley, Sergio Lago-Alves, Thomas Wu, and the participants of the Monetary Policy Seminar at the Bank of Japan Institute for Monetary and Economic Studies and the UCSC Economics Department Seminar for their comments and suggestions.

[†]Corresponding author. Department of Economics, E2, University of California, Santa Cruz, Santa Cruz, CA 95064 USA. Tel: 1 (831) 459-5733; Email: vsushko@ucsc.edu; Web: http://people.ucsc.edu/∼ vsushko/

1 Introduction

Foreign exchange returns of high (low) yield currencies tend to exhibit negative (positive) skewness – long duration of runs interrupted by abrupt crashes. Such apparent violation of the efficient market hypothesis combined with the loose fundamental anchoring of foreign exchange rates, also known as the *exchange rate disconnect puzzle* first documented by Mussa (1986) and Flood and Rose (1993), suggests that strategic behavior by traders can play an important role in exchange rate dynamics. Particularly, in a situation where traders may have private information related to future payoffs of a foreign investment, their individual actions may trigger a cascade of similar actions by other traders. Several features of carry trade make it especially susceptible to such a mechanism of chain reaction through information revelation.

Carry trade is a strategy in which an investor finances a long position in a high yield currency by borrowing in a low yield currency betting that the exchange rate will not change so as to offset the profits made on the interest rate differential.[1] Since central banks set short-term interest rates with domestic inflation considerations in mind, it allows carry traders to lock-in a profit from the interest rate differential, but the key uncertainty of an adverse exchange rate swing remains. In other words, carry traders knowingly expose themselves to foreign exchange rate risk. The profitability of their investment strategy is contingent on the violation of the uncovered interest parity (UIP) which is an ex-ante no-arbitrage condition predicting that excess returns from holding high interest rate currency must be eliminated through an expected depreciation of that currency. Plantin and Shin (2010) refer to the instant when exchange rate of high yield currency depreciatiates back to a commonly known fundamental level as "the day of reckoning".

We study the implications of this key "day of reckoning" uncertainty for strategic behavior of carry traders, and the consequences of their actions for foreign exchange volatility. Since all carry traders face a common risk, they learn about the likelihood of an adverse foreign exchange rate swing, not only from their private information, but also from the actions of others. This leads to strategic complementarity in their actions to engage in carry trade. Strategic complementarity is an important result since, as shown in a dynamic coordination game by Plantin and Shin (2010),

[1] Burnside et al. (2007) and Hochradl and Wagner (2010) document persistent excess returns to carry trade strategies.

it makes foreign exchange speculation destabilizing when coupled with the notion of "the day of reckoning." Plantin and Shin introduce strategic complementarity by the means of positive funding externality – the additional assumption that carry traders reduce funding costs for each other by exacerbating UIP violation when piling into a high yield currency. In contrast, we demonstrate that the aggregate uncertainty about the probability of the crash is by itself sufficient to make carry traders' actions strategic complements, leading to runs on the high yield currency punctuated by endogenous episodes of "explosive" carry unwinding. Furthermore, the collective unwinding in this environment is stochastic since it turns out that in equilibrium each carry trader assigns greater weight to the actions of others rather than her own private information only with a certain probability. The stochastic equilibrium outcome of our model takes from the stochastic herding approach of Nirei (2006, 2008). This gives a result similar to the *stochastic bifurcation* equilibrium dynamics of Plantin and Shin (2010), whereby a small smooth change to a parameter value can lead the system to instantly swing to a new equilibrium.[2] However, we obtain this results in a simpler setting with the underlying mechanism being a chain reaction through information revelation about currency crash risk. Leverage in our model plays a secondary role, only exacerbating the pre-existing dynamics. The impact of leverage is highly non-linear, and suggests that there may exist an optimal percentage margin requirement on speculative positions which is a function of the interest rate differential between high and low yielding currencies.

The main empirical implication of stochastic herding in carry trade relates to the distribution of rare events in foreign exchange. Whereas the central limit theorem characterizes an outcome of a simple information aggregation process, choice correlations lead to fat tail effects. In particular, the equilibrium fraction of carry traders that herd on the same action is described by a probability distribution that exhibits a power decay with exponential truncation. Thus, the mechanism of stochastic herding may explain recent findings in option pricing literature that an exponentially dampened power-law provides a better approximation to rare events in foreign exchange returns than the traditional Merton's compound Poisson normal jump process (see Wu (2006) and Bakshi et al. (2008)). Furthermore, since an exponentially dampened power-law in the distribution of rare events in foreign exchange can be observed even before the "explosive" unwinding takes place it

[2]See Bass and Burdzy (1999) for a comprehensive treatment of stochastic bifurcation processes.

potentially allows us to quantify what Rajan (2006) has dubbed the "hidden tail risk."[3]

We test the goodness of fit of the distribution derived from the model to the realized volatility jumps in JPY/USD foreign exchange rate. The Japanese yen in particular has served as a funding currency in carry trade because of a prolonged "zero interest rate" policy of the Bank of Japan. Brunnermeier et al. (2009) find that yen has exhibited the highest degree of skewness among developed countries' currencies, and attribute this to large periodic yen appreciations caused by the unwinding of carry trade. Leptokurtic features arise if standard Brownian motion in the evolution of financial returns is punctuated by periodic jumps. We examine daily jumps in the JPY/USD exchange rate extracted using a non-parametric method of bi-power variation following Barndorff-Nielsen (2004) and Barndorff-Nielsen and Shephard (2006). This method makes use of high-frequency data (five minute intervals) to take out intraday noise and isolate daily returns that evolved discontinuously (are inconsistent with Gaussian volatility component). We focus on time period from Janunary 1, 1999 through February 1, 2007, thus the 1998 and 2008 crashes are just outside of our sample.

We find that positive and negative jumps in the JPY/USD exchange rate exhibit asymmetries consistent with carry trade: higher likelihood of large discrete yen appreciations coupled with serial correlation and non-linear dependence in yen *appreciation* jumps indicate that large yen appreciations tend to occur over consecutive days and may be non-random. In contrast, yen *depreciation* jumps are best described as white noise. The asymmetries are more pronounced when there is greater incentive to engage in carry trade, a higher interest rate differential between U.S. and Japan, and when the general level of uncertainty is higher, that is higher level of option implied volatility index (VIX).

Since jumps are extracted using a non-parametric method it allows for hypothesis testing regarding the underlying distribution. We find that for yen *appreciatin* jumps a compound Poisson normal jump process, which serves as a good approximation if jumps are independent of each other, is strongly rejected in favor an exponentially dampened power-law, which is an outcome of stochastic herding by carry traders chasing information about the "crash risk." Simulation results with

[3]See for instance Jansen and de Vries (1991) and Longin (1996) who suggest that price fluctuations in normal times and rare market crashes are caused by the same mechanisms. Also, Morris and Shin (1999) argue that choice interdependence among traders must be explicitly incorporated into the estimates of "value at risk" and call for greater attention to the actions of market participants.

parameters estimated from the data confirm that the underlying data generating process is different for negative and positive jumps, with negative jumps subject to more extreme fluctuations. The contrast between simulation results of yen appreciation (negative) and yen depreciation (positive) jumps clearly captures the origins of the negative skewness of JPY/USD returns.

Finally, parametric restrictions from the model allow us to identify economic factors that lead to extreme volatility by intensifying the herd effect. In the analysis of subsamples we find that the key distribution parameter that captures the intensity of herding is higher during times of greater interest rate differential and higher values of VIX. Fitting the model in reduced form to the data, we find that higher level of speculative futures positions increases the "tail risk" directly, while lower margin requirements and higher option implied risk premia raise the likelihood of sharp yen appreciation only jointly with an accumulated carry position in the market. The impact of the volume of speculative futures on the "tail risk" is particularly robust, corroborating the key hypothesis that carry trade considerations play a destabilizing role in foreign exchange markets, even in periods not punctuated by "extreme crashes," such as the LTCM or the subprime episodes.

The study is organized as follows. Section 2 empirically motivates the key assumption of the model that "the day of reckoning" risk plays a central role in carry trade. Section 3 overviews related herding literature contrasting herding due to informational cascades and the stochastic herding mechanism employed in this paper. Section 4 presents the model. Section 5 tests the model and examines the link between JPY/USD exchange rate volatility and carry trade. Section 6 concludes.

2 Evidence of the "Day of Reckoning" Fears in Yen Carry Trade

The top two panel of Figure 1 show the JPY/USD exchange rate and the U.S.-Japan interest rate differential from Januray 1, 1999 through February 1 2007. In strong violation of the UIP an increase in the interest rate spread corresponded with dollar appreciation against the yen in late 1999 through 2000 and again from 2004 through 2007.[4] For instance, Ichiue and Koyama (2008) estimate the UIP regression coefficient as low as -2.79 for the yen.[5] In line with a "peso"

[4] An appreciation of the high yield currency is an example of the forward premium puzzle and the violation of the uncovered interest parity (UIP) well documented by Hansen and Hodrick (1980) and Engel (1996).

[5] Under rational expectations a regression of exchange rate returns on in interest rate differential should yield a coefficient of 1.

type problem, Farhi et al. (2009) interpret UIP violations as a compensation to carry traders for bearding the risk of periodic currency crashes, such as sharp yen appreciation in 2008 following the sub-prime crisis. The third panel of Figure 1 shows that this rise in ex-ante carry trade returns was accompanied by a decrease VIX, perhaps associated with a global search for yields during the 2000s. Finally, the bottom panel of Figure 1 shows that the dramatic rise in returns to JPY/USD carry trade in the 2004 through 2006 period was accompanied by an increase in non-commercial yen short futures positions on The Chicago Mercantile Exchange (CME), which are a common proxy for carry trade activity (see Klitgaard and Weir (2004), Galati, Heath and McGuire (2007), Brunnermeier et al. (2009) and Cecchetti et al. (2010)). Combined, these trends suggest that carry trade may have been a major factor in JPY/USD exchange rate dynamics during our sample period.

Figure 1 [about here]

Figure 2 shows the relationship between the market price of risk of large yen appreciation (as proxied by risk reversals[6]) and CME net non-commercial short yen futures positions (percent of total open interest). Risk reversals are options contracts used to hedge against the risk of substantial unidirectional price movement, and as such their values are often treated as a proxy for market expectations about sharp yen appreciation.[7]

Figure 2 [about here]

The negative values of risk reversals depicted in Figure 2 indicate higher implied volatility on extreme yen *appreciation* side during the entire 2004-2006 period. In other words, the overall market was hedging against sharp yen appreciation during the height of the yen carry trade. Moreover, note the close association between risk reversals and net speculative short positions in yen: when risk reversals become more negative (higher market expectation of sharp yen *appreciation*) net speculative futures positions decline. In order to test whether carry traders respond to the market value of the risk of sharp yen appreciation we repeat the exercise of Hutchison and Sushko (2010) who find that risk reversals Granger-cause speculative futures positions in yen.

[6] A risk reversal is a hedge against a large price movement in one direction constructed by a simultaneous purchase of deep out-of-money call and sale of deep out-of-money put option (usually 25 or 10 delta) of the same maturity (or vise-versa). The value itself is the implied volatility for the call minus the implied volatility of the put. For detailed guide to risk reversals see Galati, Higgins, Humpage and Melick (2007).

[7] Gagnon and Chaboud (2007) find that prices of deep out-of-money foreign exchange options indicate an overall market hedge against large yen appreciation and Farhi and Gabaix (2008) show that under certain conditions risk reversals contain information on currency"disaster risk premia"

Table 1 [about here]

Table 1 reports the results of the Granger-causality test between yen risk reversals (RRs) and net non-commercial yen short futures positions (NCMS). Risk reversals Granger-cause NCMS under both 1 and 2 lag specifications and this effect is significant at 1 percent level. Furthermore, the effect is robust to controlling for the exchange rate, indicating that risk reversals contain important information to carry traders on the currency risk of their positions, supporting the notion that "day of reckoning" considerations are central to carry trade.

3 Stochastic Herding and Related Literature

Related arbitrage literature includes Abreu and Brunnermeier (2002, 2003) who model a continuous time coordination game in which the market finally crashes when a critical mass of arbitrageurs synchronizes their trades. The coordination element coupled with information asymmetries create an incentive for fully rational investors to base their actions on the actions of others, i.e. herd. Scharfstein and Stein (1990), Bikhchandani et al. (1992), Banerjee (1992), and Avery and Zemsky (1998) have formulated a theory of informational cascades, a type of herding that takes place when agents find it optimal to completely ignore their private information and follow the actions of others in a sequential move game.[8] Because players select their actions sequentially, the system will eventually but unexpectedly swing from one stable state to another. In contrast, in our framework herding is stochastic, following Nirei (2006, 2008) with some foundation going back to probabilistic herding in the famous ant model of Kirman (1993).[9] Only a fraction of agents synchronize, the size of the fraction in turn depends on the realization of private signals. Stochastic unwinding of carry trades emerges because strategic complementarity makes it optimal for some agents to place a higher value on the informational content of the actions of others relative to their own private signals. This setup differs from pure informational cascades, and is similar to Gul and Lundholm (1995), in that in our case, as in theirs, none of the information goes unused. Because herding is stochastic so too is the transition between equilibria yielding *stochastic bifurcation* dynamics of

[8] See Chari and Kehoe (2004) for the application of information cascades to financial markets.

[9] Alfarano et al. (2005, 2008) also show that the Kirman-type mechanism can match higher moments in financial returns, such as volatility clustering and Pareto tails. However, whereas in Alfarano, Lux, and Wagner the key herding effect is exogenous, we show that herding arises endogenously in a microfounded rational expectations equilibrium with information asymmetries.

Plantin and Shin (2010).

The resulting probability distribution of the fraction of carry traders who unwind their positions is derived from the threshold rule governing their actions. This is similar to the threshold-based switching strategy employed by Morris and Shin (1998) in the Global Games approach. However, unlike the Global Games, the threshold value of the signal determining whether or not a carry trader chooses to unwind fluctuates endogenously with the actions of other carry traders. Endogenously fluctuating threshold can generate cascading behavior whereby agents continuously raise their minimum threshold belief for unwinding as they observe more and more unwinding around them. In this manner, we show that even if the probability of the "day of reckoning" is trivially small, in equilibrium there is a non-trivial possibility of an episode of "explosive" carry trade unwinding. The resulting aggregate action will follow a highly non-normal distribution implying stylized facts such as skewness and fat tails in foreign exchange returns.

4 Model

4.1 Threshold Strategy for Carry Trade Unwinding

There are N informed risk neutral traders indexed by $i = 1, 2, \ldots, N$. Each trader can engage in a carry trade where she goes short in yen and long in dollars. Let $\Delta s > 0$ denote dollar appreciation and $\delta \equiv i - i^* > 0$ denote the interest rate differential between U.S. and Japan. Carry traders profit from UIP violation $(\Delta s + \delta) > 0$.

The return to carry trade is stochastic because exchange rate returns, Δs, are subject to crash risk. There are two state of the world. "High" and "Low," and Δs takes from two values, Δs_H and Δs_L, depending on the realization of the state, where $(\Delta s_H + \delta) > 0 > (\Delta s_L + \delta)$. We can think of the realization of "Low" state as the "day of reckoning" following Duffie et al. (2002), when the dollar return to holding an asset snaps back to a commonly known fundamental value.

Suppose that each trader has an existing carry position, $k > 1$, and one new addition of funds in yen. Traders maximize $E(\Delta s + \delta)k'$ by choosing k'. Since traders are risk neutral the optimal position is either $k' = k + 1$ or $k' = 0$. We call the trader's choice $k + 1$ as "stay," and 0 as "exit" of the carry trade.

Let m denote the number of exiting traders. We assume that exchange rate returns depend on

the extent of the net outflow of funds from the carry currency. Thus Δs is a decreasing function of $mk - N + m$, where mk is the unwound amount of carry trades by exiting traders and, $N - m$ is the increase in the carry position by continuing traders. Each trader submits to a market maker her supply schedule, namely "stay" or "exit," conditional on m. The market maker then chooses m so that the number of the exiting traders coincides to the chosen m.

Each trader draws a private signal x_i, which is correlated with the state. The distribution of x_i is a common knowledge, where x_i is drawn from F if the true state is High and from G if the true state is Low. Let f and g denote the density functions of F and G, respectively. We assume that the odds ratio $f(x)/g(x)$ is increasing in x. Namely, F and G satisfy the monotone likelihood ratio property (MLRP). This assumption implies that a larger value of x conveys the information that it is more likely that the state is High rather than Low.

We conjecture that each trader employs a threshold strategy in which trader i stays in carry ($k' = k + 1$) if $x_i > \bar{x}$, and exits ($k' = 0$) otherwise. For a fixed m, a staying trader must be indifferent between stay or exit if she draws a private information at the threshold level $\bar{x}(m)$.

Thus $\bar{x}(m)$ must satisfy the indifference condition:

$$E(\Delta s + \delta \mid m, x_i = \bar{x}(m)) = 0. \tag{1}$$

Then,

$$(\Delta s_H + \delta)\Pr(\text{High} \mid x_i = \bar{x}(m), m) + (\Delta s_L + \delta)\Pr(\text{Low} \mid x_i = \bar{x}(m), m) = 0, \tag{2}$$

where "Pr" denotes a likelihood function. Equivalently, the threshold $\bar{x}$ is determined by the following equation:

$$\log \frac{\Pr(\text{High} \mid x_i = \bar{x}(m), m)}{\Pr(\text{Low} \mid x_i = \bar{x}(m), m)} = \log \frac{-\Delta s_L - \delta}{\Delta s_H + \delta}. \tag{3}$$

First, we note that:

$$\frac{\Pr(\text{High} \mid x_i = \bar{x}(m), m)}{\Pr(\text{Low} \mid x_i = \bar{x}(m), m)} = \frac{\Pr(\text{High}, x_i = \bar{x}(m), m)}{\Pr(\text{Low}, x_i = \bar{x}(m), m)}, \tag{4}$$

$$= \frac{\Pr(x_i = \bar{x}(m) \mid \text{High}, m)}{\Pr(x_i = \bar{x}(m) \mid \text{Low}, m)} \frac{\Pr(m \mid \text{High})}{\Pr(m \mid \text{Low})} \frac{\Pr(\text{High})}{\Pr(\text{Low})}, \tag{5}$$

$$= \frac{f(\bar{x}(m))}{g(\bar{x}(m))} \left(\frac{F(\bar{x}(m))}{G(\bar{x}(m))}\right)^m \left(\frac{1 - F(\bar{x}(m))}{1 - G(\bar{x}(m))}\right)^{N-1-m} \theta_0, \tag{6}$$

where θ_0 denotes the prior likelihood ratio, which is the prior belief on High divided by the prior belief on Low state. The term F/G expresses the likelihood ratio inferred by m exiting traders, and the term $(1-F)/(1-G)$ is the likelihood ratio inferred by staying traders. because the equation is based on the indifference condition for a staying trader and her own information is already included by the term f/g, we only count $N-1-m$ staying traders in this term. From equation (6), it is straightforward to show the optimality of the threshold rule: only if a trader draws an information greater than the threshold, i.e. $x_i > \bar{x}$, the left hand side of (3) exceeds the right hand side due to the MLRP, would the trader chooses to stay in carry.

The threshold rule has the following property.

Proposition 1. *The threshold function $\bar{x}(m)$ is increasing in m.*

Proof: See Appendix A.

Then we obtain:

$$\frac{d\bar{x}}{dm} = \frac{-\log\frac{F(\bar{x})}{G(\bar{x})} + \log\frac{1-F(\bar{x})}{1-G(\bar{x})} + \frac{(\Delta s_L - \Delta s_H)(k-1)\Delta s'}{-(\Delta s_H + \delta)(\Delta s_L + \delta)}}{\frac{f'(\bar{x}) - g'(\bar{x})}{f(\bar{x})/g(\bar{x})} + m\left(\frac{f(\bar{x})}{F(\bar{x}))} - \frac{g(\bar{x})}{G(\bar{x})}\right) + (N-1-m)\left(\frac{g(\bar{x})}{1-G(\bar{x})} - \frac{f(\bar{x})}{1-F(\bar{x})}\right)}$$
$$> 0 \tag{7}$$

This implies that traders' decisions exhibit strategic complementarity: when a trader decides to exit, it increases m and then $\bar{x}$, making other traders more likely to exit.

4.2 Equilibrium

We define an equilibrium as a mapping from a profile of realized private information (x_i) to an action profile with m "exits" and $N-m$ "stays", such that the number of traders with $x_i < \bar{x}(m)$

coincides with m for each realization (x_i). The equilibrium notion here is a standard rational expectations equilibrium in a market microstructure with a market maker and traders submitting supply schedules (Vives (2008)).

Next, following Nirei (2006, 2008), we characterize the equilibrium by constructing a fictitious tatonnement process. We imagine that the market maker finds an equilibrium m as follows. At the initial step $s = 0$, the market maker starts with $m_{s=0} = 0$ and counts the number of traders who would exit according to their supply schedules given the information $m = 0$. If no trader exits, then the process stops here and $m = 0$ is chosen as an equilibrium. If $n_{s=0} > 0$ traders choose to exit, the step is increased to $s = 1$, and $m_{s=1}$ is set by $m_s = m_{s-1} + n_{s-1}$. If no traders other than the traders who chose to exit previously decide to exit, then the process stops and $m = m_s$ is chosen as an equilibrium. Otherwise, the step is increased and the process iterates until it stops. Nirei (2006) has shown that this procedure always converges to an equilibrium, m, and the selected equilibrium is the smallest among potential equilibria.

The fictitious tatonnement process, m_s, $s = 0, 1, \ldots$, can be embedded to a stochastic process defined in the probability space of the private information profile (x_i). Namely, we can derive the probability distribution of m_{s+1} conditional on m_s before the realization of x_i. It is shown (Nirei (2006)) that n_s follows a branching process in which the number of "children" born by a "parent" in step s follows a binomial distribution with a probability parameter p_s and population $N - m_s$, and if we increase N to infinity, the binomial asymptotically converges to a Poisson distribution with mean $\mu_s = \lim_{N\to\infty} p_s(N - m_s)$.

This property of the fictitious tatonnement process is utilized to characterize the equilibrium. The equilibrium m is the sum of n_s over s, the total number of "children" born in the branching process until it stops. Then, we can apply a powerful theorem by Otter (see Harris (1989)). Consider a branching process n_s, in which the mean number of children per parent is constant at μ, and the initial condition is $n_0 = 1$. Then the total population, $m = \sum_s n_s$, follows a dampened power-law distribution in the tail:

$$\begin{aligned} \Pr(m \mid m_0 = 1) &\sim m^{-1.5}(\mu e^{1-\mu})^m \\ &= C_0 m^{-1.5} e^{-\phi m} \end{aligned} \tag{8}$$

for a large m, where ϕ is a constant determined by the distribution of the number of children per parent. In our case, where the number of children follows a Poisson distribution, we further have $\phi = \mu - 1 - \log \mu$ for the case of $\mu < 1$ (Nirei (2006)). The key parameter for the fluctuation of m is μ. When $\mu \leq 1$, the fictitious tatonnement n_s is a supermartingale, which stops in a finite step, and whose total population m is finite with probability one. Equation (8) and the relation between ϕ and μ implies that the mean and variance of m is determined by μ. A greater μ decreases ϕ and thus makes the exponential truncation point further in the tail of (8). $\mu = 1$ is the critical point at which (8) reduces to a pure power law distribution with indefinite mean. Thus, we observe that the model is capable of generating a substantial size of fluctuations in m when μ is close to 1. When μ is greater than 1, the fictitious tatonnement is "explosive" and there is a positive probability in which the process does not stop in a finite step. In our finite model, this event corresponds to the case, $m = N$.

In our model, μ_s is not constant over the tatonnement step s. However, we can infer the range of μ_s as follows. Suppose that the true state is "Low." For a large N, the mean number of traders who are induced to unwind the carry by observing an additional trader unwinding to the existing unwinding traders m is approximated by:

$$\mu_s \sim (N - m_s) g(\bar{x}(m_s)) / (1 - G(\bar{x}(m_s))) (d\bar{x}(m_s)/dm), \tag{9}$$

where $d\bar{x}/dm$ is the increase in the threshold, $g/(1-G)$ is the conditional density at the threshold level (i.e. the hazard rate), and $N - m_s$ is the number of staying traders at step s. Then,

$$\mu_s = \lim_{N\to\infty} \frac{-\log \frac{F(\bar{x}_s)}{G(\bar{x}_s)} + \log \frac{1-F(\bar{x}_s)}{1-G(\bar{x}_s)} + \frac{(\Delta s_L - \Delta s_H)(k-1)\Delta s'}{-(\Delta s_H + \delta)(\Delta s_L + \delta)}}{\frac{1}{N-m} \frac{f'(\bar{x}_s) - g'(\bar{x}_s)}{f(\bar{x}_s)/(1-G(\bar{x}_s))} + \frac{m}{N-m} \left(\frac{f(\bar{x}_s)/g(\bar{x}_s)}{F(\bar{x}_s)/(1-G(\bar{x}_s))} - \frac{1-G(\bar{x}_s)}{G(\bar{x}_s)} \right) + \frac{N-1-m}{N-m} \left(1 - \frac{f(\bar{x}_s)/g(\bar{x}_s)}{(1-F(\bar{x}_s))/(1-G(\bar{x}_s))} \right)}, \tag{10}$$

where $\bar{x}_s$ is a short-hand for $\bar{x}(m_s)$. For a fixed, finite m_s, we have:

$$\mu_s = \frac{-\log \frac{F(\bar{x}_s)}{G(\bar{x}_s)} + \log \frac{1-F(\bar{x}_s)}{1-G(\bar{x}_s)} + \frac{(\Delta s_H - \Delta s_L)(k-1)\Delta s'}{(\Delta s_H + \delta)(\Delta s_L + \delta)}}{1 - \frac{f(\bar{x}_s)/g(\bar{x}_s)}{(1-F(\bar{x}_s))/(1-G(\bar{x}_s))}}. \tag{11}$$

Note that:

$$\frac{-\log\frac{F(\bar{x})}{G(\bar{x})}+\log\frac{1-F(\bar{x})}{1-G(\bar{x})}}{1-\frac{f(\bar{x})/g(\bar{x})}{(1-F(\bar{x}))/(1-G(\bar{x}))}}=\frac{\log\frac{f(\bar{x})/g(\bar{x})}{F(\bar{x})/G(\bar{x})}-\log\frac{f(\bar{x})/g(\bar{x})}{(1-F(\bar{x}))/(1-G(\bar{x}))}}{1-\frac{f(\bar{x})/g(\bar{x})}{(1-F(\bar{x}))/(1-G(\bar{x}))}}>1. \tag{12}$$

Thus, the fictitious tatonnement starts out as an explosive process near $m_s/N = 0$.

For a range of larger values of m_s, we can characterize μ as follows. Consider an alternative continuum version of our model in which there are a continuum of traders rather than finite N traders. Then, by the law of large numbers, we expect that the equilibrium fraction of exiting traders to be $G(\bar{x})$. Thus, we impose $m/N = G(\bar{x}(m))$ in the expression (10). Then:

$$\mu_s \approx \Lambda_1(\bar{x}) + \Lambda_2(\bar{x}) \times \frac{(\Delta s_H - \Delta s_L)(k-1)\Delta s'}{(\Delta s_H + \delta)(\Delta s_L + \delta)}, \tag{13}$$

where:

$$\Lambda_1 \equiv \frac{-\log\frac{F(\bar{x})}{G(\bar{x})}+\log\frac{1-F(\bar{x})}{1-G(\bar{x})}}{\frac{f(\bar{x})/g(\bar{x})}{F(\bar{x})/G(\bar{x})}-\frac{f(\bar{x})/g(\bar{x})}{(1-F(\bar{x}))/(1-G(\bar{x}))}}, \tag{14}$$

and

$$\Lambda_2 \equiv \frac{1}{\frac{f(\bar{x})/g(\bar{x})}{F(\bar{x})/G(\bar{x})}-\frac{f(\bar{x})/g(\bar{x})}{(1-F(\bar{x}))/(1-G(\bar{x}))}}. \tag{15}$$

Thus Λ_1 takes a value greater than 1 when $\bar{x}$ is small (and thus m is small) by the argument in Equation (12), whereas it takes a value less than 1 when $\bar{x} \to \infty$ (and thus $m \to N$). Thus, we can infer that μ_s travels from an explosive region to a dampening region (if k is small enough) as the fictitious tatonnement develops into a larger m. This suggests that the tatonnement generates m smaller than N when N is large enough, and the fluctuation of m follows the dampened power-law distribution.

To summarize, in the absence of strategic complementarity, a random realization of signals x_i about "High" or "Low" state would have induced some traders to unwind independently of one another. Then, at the completion of the tatonnement process the total population of unwinding traders m would have been drawn from a Poisson distribution with mean μ_1. For $N \to \infty$ the sum of Poisson events converges to a Normal distribution. On the other hand, chasing the common information about "the day of reckoning" introduces strategic complementarity. Then, an initial "independent" unwinding action drawn from a Poisson distribution with mean μ_1 triggers a chain reaction (a branching process) with intensity μ that stops in finite time for $\mu < 1$. As a result, m

will be drawn from a population distribution that exhibits a power-law with exponential truncation in the tail, with the speed of exponential truncation, ϕ, inversely related to μ.

4.3 Leverage

In addition to issuing liabilities in low-interest currencies, carry trade can be conducted using currency forwards and futures on the margin (Gagnon and Chaboud (2007)), since as long as covered interest parity (CIP) holds a long dollar short yen currency futures position profits from the UIP violation much like a long dollar bond short yen bond position.[10]

Let $0 < M \leq 1$ denote the margin requirement, such that $M = 1$ means that 100 percent of the dollar asset purchase must be financed by the trader's funds. Trading on the margin allows for leveraged positions. To simplify notation, assume that the interest rate in low yielding currency is approximately zero: $i^* \approx 0$. Then a carry trader who maximizes the expected value of next period's wealth faces the following budget constraint:

$$w' = (w - k') + \frac{1}{M} E(\Delta s + \delta) k', \tag{16}$$

where w denotes current wealth of which k' is invested in carry trade on the margin. The threshold condition (1) becomes:

$$E(\Delta s + \delta \mid m, x_i = \bar{x}(m)) = M. \tag{17}$$

Equation (17) illustrates the mitigating effect of a higher margin requirement. Since the return to carry trade must now cover the opportunity cost of foregone alternative uses of a trader's initial wealth, which she has instead pledged as collateral for carry trade, a higher margin requirement raises the required expected rate of return to satisfy the threshold rule. In equilibrium the intensity of the branching process, μ_s, depends on M in a complex non-linear fashion:

$$\mu_s \approx \Lambda_1(\bar{x}) + \Lambda_2(\bar{x}) \times \frac{(\Delta s_H - \Delta s_L)(k-1)\Delta s'}{(1 + \delta - M)(\Delta s_H + \Delta s_L) + (\delta - M)^2}. \tag{18}$$

Equation (18) shows that the effect of M on μ_s is determined by the relative value of the

[10] For evidence that the devations from CIP are rare and insignificant see for example Burnside et al. (2008).

percentage margin requirement to the percentage interest rate differential, δ. When M is close to 1, the denominator on the RHS of (18) is large, mitigating the effect of expected crash risk, $(\Delta s_H - \Delta s_L)$, and accumulated carry positions, k, on μ. On the other hand, when M approaches zero from above, especially when it falls below the value of δ, the denominator becomes small, magnifying the impact of crash risk and carry trade volume on μ_s.

Figure 3 [about here]

Figure 3 shows the relationship between the margin requirement and μ, holding other parameters constant. We set the interest rate differential equal to 4 percent and yen depreciation equal to 5 percent in "High" state and -4 percent in "Low" state. Total carry position is set at $k = 100,000$ units. The figure shows that when the margin requirement is high a reduction in margin requirement has virtually no effect on the intensity of the branching process measured by μ (herding). However, when the margin requirement is lowered below a certain threshold (in this case approximately 20 percent), then the branching process begins to intensify exponentially. Since μ is inversely related to the degree of exponential truncation in the tail of the distribution of m, a higher μ necessarily implies a thicker tail in the probability distribution of aggregate action, and hence more extreme volatility. Moreover, when the margin requirement reaches the second threshold (in this case approximately 10 percent) then μ is suddenly taken from subcritical ($\mu < 1$) to superctitical state ($\mu > 1$), implying an "explosive" episode of coordination on the same action (all carry trader unwind).[11]

4.4 Exchange Rate

The function $\Delta s(mk - N + m)$ is constructed such that the dynamic pattern of exchange rates matches with the model when the static equilibrium of the model is repeated with evolving currency position k. Consider the case $k_0 = 0$. Then the effect of Δs on μ in (10) is negative, and thus we expect a high probability for staying behavior: $k' = 1$. In the next period, we set $k_1 = k' = 1$. We have a greater value of μ_s, and expect some probability of collective unwinding. When k becomes quite large, we expect an even higher probability of sudden unwinding because of a greater μ_s. Thus,

[11] In a related study, Nirei and Sushko (2010) use highly disaggregated institutional investor portfolio data to show that the transition to the broad sell-off of U.S. equities by institutional investors in the summer of 2007 is consistent with a massive coordination episode as μ travels from a subcritical to a superctirical state.

we expect a small value of m and a gradual increase of k over periods, whereas the development of the carry accumulation is punctuated by a "sudden fall" when m takes some large positive value. In terms of the exchange rate, the currency appreciation Δs is a negative function of $mk - N + m$, and thus the dynamics of m corresponds to the long periods of gradual appreciation of the dollar punctuated by sudden crashes.

5 Evidence from Stochastic Volatility in the JPY/USD Exchange Rate

5.1 Data

We use intraday JPY/USD exchange rate data from Olsen and Associates. The data was collected from commercial banks by Tenfore and Oanda, and covers the January 1, 1999 to February 1, 2007 time-period. The data consists of the bid and the offer spot exchange rate at the end of every 5-minute interval over every 24-hour period. The quotes are indicative quotes, i.e. not necessarily traded quotes. In addition we construct a daily series of the interest rate spread between U.S. and Japan as the difference between the effective federal funds rate and Japan's uncollateralized overnight call rate, which are publicly available from the Federal Reserve Bank of New York and Bank of Japan respectively. Finally, we obtain daily data on the S&P 500 options implied volatility index (VIX) from Wharton Research Data Services (WRDS).

Figure 4 [about here]

The left panel of Figure 4 shows the normal kernel density plot of the JPY/USD exchange rate log-return series for our sample period. The leptokurtic features are apparent, with a fatter negative tail (yen appreciations). The right panel shows the associated quantile-quantile plot against a normal distribution (red line). Again, the negative tail exhibits a larger deviation from the normal hypothesis and has a higher number of data points in the extreme range. In the remaineder of the section we provide statistical and economic analysis to better understand the underlying data generating process of these extreme realizations in the tails of the distribution of JPY/USD returns.

5.2 Extracting Jumps Using Bi-Power Variation

Consider a jump diffusion process for the evolution of foreign exchange rate returns:

$$ds(t) = \mu(t)dt + \sigma(t)dW(t) + \kappa(t)dJ(t), \tag{19}$$

where $s(t)$ is log exchange rate, $\mu(t)$ is drift, $\sigma(t)$ represents Gaussian volatility component, and $W(t)$ is standard Brownian motion such that $dW(t) = \sqrt{dt}dz$ with $dz \sim N(0,1)$. The last term on the RHS represents the stochastic jump process, $\kappa(t)$ is the size of jump at time t and $dJ(t)$ is an indicator of jumps; $dJ(t) = 1$ with probability $\lambda(t)dt$ and 0 otherwise. A standard practice is to assume that jumps are independent of one another, and therefore to model their arrival rates with a Poisson process where $\lambda(t)$ would correspond to a Poisson arrival rate. In contrast, we do not make any parametric assumptions about $\kappa(t)$. Instead we use a non-parametric method of bi-power variation of Barndorff-Nielsen (2004) to estimate daily jumps as the difference between the total intra-day realized volatility, $RV_t(\Delta)$, and its continuous component, $BV_t(\Delta)$. $RV_t(\Delta)$ is the sum of square intraday discretely sampled Δ -period returns between time 0 and time t. If the intraday data is obtained at five minute intervals then $1/\Delta = 288$ is the number of daily data points. Barndorff-Nielsen (2004) show that in the limit (as $\Delta \to 0$) realized daily volatility approaches the continuously aggregated sum of square returns. Since returns from two adjacent intraday sample points share the persistent volatility but not the sporadic jumps, it follows that bi-power variation provides a reasonable proxy for the persistent component of the volatility:

$$BV_{t+1}(\Delta) \to \int_t^{t+1} \sigma^2(s)ds, \tag{20}$$

as $\Delta \to 0$.

Since realized volatility, $RV_{t+1}(\Delta)$, and bi-power volatility, $BV_{t+1}(\Delta)$, can be directly calculated from the observed returns, it follows that the jump component can be approximated as the difference of the two:

$$RV_{t+1}(\Delta) - BV_{t+1}(\Delta) \to \sum_{t<s\leq t+1} \kappa^2(s), \tag{21}$$

where positive and negative jumps are indexed according to the direction of the corresponding daily return: $\kappa_+(t+1) = I_{\Delta s(t+1)>0} \sum_{t<s\leq t+1} \kappa^2(s)$ and $\kappa_-(t+1) = I_{\Delta s(t+1)<0} \sum_{t<s\leq t+1} \kappa^2(s)$, with $I_{(\cdot)}$ representing an indicator function for positive and negative daily returns respectively. We take additional steps to account for the finite sample bias, and in addition to reporting all jumps, we report jumps estimated with $\alpha = 0.05$ and 0.01 significance levels correcting for intraday noise. Choosing to estimate fewer but more probable jumps as opposed to a continuous adjustment amounts to choosing a lower significance level α associated with critical value Φ_α. The details of this procedures are outlined in Appendix B.1.

5.3 Descriptive Statistics and Serial Correlation in Yen Appreciation Jumps

Table 2 shows jump summary statistics. Mean absolute values of jumps in yen appreciations are higher for all α ranging between 0.019 and 0.044, compared to 0.16 and 0.36 for jumps in yen depreciations. Negative jumps (appreciations) also exhibit higher kurtosis. The maximum jump in appreciation is 2.959 compared to the maximum jump of 1.482 in yen depreciation. The last row of Table 2 reports Ljung-Box test statistic for white noise. Negative jumps exhibit a high degree of serial correlation with the Q-stat in the 133.5 to 161.9 range. Using a more restrictive $\alpha = 0.01$ criteria serial correlation is rejected for positive jumps selected. Overall, Table 2 indicates that jumps in yen appreciation are more rare than jumps in yen depreciation, but tend to be larger in magnitude and occur over several consecutive days, implying an element of predictability.

Table 2 [about here]

5.4 Sample Split by U.S.-Japan Interest Rate Differential and the VIX

Next we split the sample by the interest rate differential between U.S. and Japan, and by the level of VIX, focusing on $\alpha = 0.01$ jumps. If carry trade plays a significant role in the stochastic volatility of the JPY/USD exchange rate then the contrast between yen appreciation and yen depreciation jumps should be magnified when the incentive to engage in carry trade is high (high interest rate differential) and when overall market uncertainty is high (high level of VIX). Based on the historical time-series in Figure 1 we observe roughly two regimes in the interest rate differential and VIX. Throughout our sample period Japan maintained a zero-interest rate policy, while the dot-com

collapse in the U.S. resulted in monetary easing beginning in late 2000, and the interest rate differential between the two countries fell to the level between 1 and 2 percent where it remained until the Fed began raising rates in 2004. Also, beginning in early 2003, the VIX settled at levels below 20 and exhibited a lower volatility. Therefore, we select 2 percent as the cutoff for the interest rate differential and 20 points as the cutoff for VIX (dashed lines).

Table 3 [about here]

Table 3 shows the associated statistics. Mean and maximum values for κ_- (yen *appreciation* jumps) are higher when the interest rate differential is high, 0.124 compared to 0.093 and 1.386 compared to 1.124 respectively. The difference is more pronounced when compared across subsamples split by VIX. When VIX is high κ_- mean and maximum are 0.140 and 1.386 compared to 0.078 and 0.510 when VIX is low respectively. In contrast, κ_+ (yen *depreciation* jumps) do not exhibit a higher mean or maximum when the differential is high, and only slightly higher mean when VIX is high, 0.099 compared to 0.082. Also, unlike yen appreciation jumps, the jumps in yen depreciation exhibit no serial correlation. Overall, the comparison of summary statistics for jumps in realized volatility across different levels of the interest rate differential and VIX are consistent with the hypothesis that carry trade plays a role in the stochastic volatility in JPY/USD.

5.5 Non-Linear Dependence in Yen Appreciation Jumps

Next we test for non-linear dependence in the jump series using the BDS test named after Brock, Dechert, and Scheinkman (1987). The BDS test can be thought of as non-linear counterpart of the Q-test.[12] The test was applied to find evidence of conditional heteroskedasticity in foreign exchange rate returns by Hsieh (1989), who found that nonlinearity in the return series entered through changing volatility. We are able to examine whether discrete changes in realized volatility exhibit non-linearity. The test embeds the time series of $\kappa(t)$ into m-dimensional vectors with overlapping entries, and computes the spatial correlation among the points in the m-dimensional space which are within tolerance radius ϵ of each other. Properly adjusted for the sample size and specially defined mean and variance, the correlation statistic asymptotically follows a standard normal distribution. We select m in the same way as the number of lags for the Q-test. In addition,

[12]For detail see Brock et al. (1996).

we parametrize the test to maintain robustness to unusual or unknown distributions of the series: we choose the tolerance radius such that 0.7 of the total number of pairs of points in the sample lie within ϵ, and the $p-values$ are computed by bootstrapping based on 1,000 repetitions. Table 4 shows the results.[13] After a minimal correction for itraday noise is employed (such as $\alpha = 0.05$) non-linear dependence is present only in yen appreciation jumps, and significant at 1 percent level for all m.

Table 4 [about here]

The BDS and the Q-test results indicate that yen *appreciation* jumps exhibit both serial correlation and non-linear depedence while the null of white noise cannot be rejected for yen *depreciation* . It follows that yen appreciation jumps exhibit an element of predictability and clustering while yen depreciation jumps are random noise. What this suggests is that continuous trends of yen depreciations (with purely random occasional jumps) were on occasion interrupted by sharp yen appreciation jumps whose persistency is clearly outside the domain of Guaissian noise.

5.6 Exponentially Dampened Power-law in the Distribution of Jumps

Quintos et al. (2001) and Candelon and Straetmans (2006) inspect the tail behavior of foreign exchange returns non-parametrically with the inference based on distribution quantiles. In contrast, the equilibrium of stochastic herding yields parametric restrictions on the tail distribution. Interestingly, it matches the empirical findings in options literature (Wu (2006)) that descrobes the Levy density of jump components, κ, as an exponentially damped power-law:

$$Pr(\kappa) \propto \begin{cases} \kappa^{-\zeta_+} e^{-\phi_+ \kappa} & , \kappa > 0 \\ |\kappa|^{-\zeta_-} e^{-\phi_- |\kappa|} & , \kappa < 0 \end{cases}$$

This specification is parsimonious enough to nest several families of jump processes. For instance the values of the power exponent $1 \leq \zeta < 3$ favor a Levy regime implying fat tails and undefined second moment while $\zeta > 3$ favors a Gaussian regime with finite variance.[14] Nirei (2006, 2008)

[13] We also run the BDS test for jump series before separating into positive and negative samples to find strong evidence of non-linear dependence. The results reported in the paper show that the time-series non-linearity comes from yen appreciation jumps.

[14] In a panel study of different currencies Bakshi et al. (2008) estimates parameters of a jump diffusion processes

shows that an exponentially dampened power-law in the distribution of rare events arises in the environment characterized by periodic episodes of coordination in traders' actions. Hence, putting the above structure on the tail ultimately allows us to make inferences about the underlying data generating process.

In order to examine whether the tail distribution of κ follows a power-law we follow the methodology of Clauset et al. (2009). For each possible choice of cutoff values for the power-law tail in the distribution of κ, we estimate the power exponent via the maximum likelihood and calculate the Kolmogorov-Smirnov (KS) goodness-of-fit statistic. We then select the minimum cutoff, κ_{min}, that gives the minimum KS-statistic. Figure 5 shows the probability plots for positive and negative jumps for each level of significance on a log-log scale. The fitted straight line on the log-log probability plot indicates that distributions of jumps exhibit strong power-law tails.

Figure 5 [about here]

Next we examine whether the power-law tails in yen *appreciation* jumps are subject to exponential truncation as stipulated by the model. Table 5 shows exponentially dampened power-law parameter estimates for negative jumps selected at three different significance levels against the two alternatives: Pareto (pure power-law) and lognormal (an alternative of random noise) distributions. Given that the distribution parameters are estimated from a relatively small number of observations in the tail we use The Bayesian Markov Chain Monte-Carlo (MCMC) method to estimate the fitted parameter uncertainty for the exponentially dampened power-law. Details of this procedure are provided in Appendix B.2.

Table 5 [about here]

The log likelihood values indicate that the exponentially dampened power-law is the preferred model for all three negative jump series. This is confirmed by the Akaike information criteria (AIC) and AIC corrected for small sample size (AICc). The estimates of ζ tend to decline as only significant jumps are selected, tending towards the borderline case of $\zeta = 2$. The estimates of the

with exponentially dampened power-law. They do not have observations on jumps separately, so they estimates ζ and ϕ for positive and negative jumps as a part of a richer parametrization scheme for the entire return process. Our study is the first to examine the goodness-of-fit of exponentially damped power-law model to empirical observations of jumps.

power-law exponent ζ in the neighborhood of 2 indicate that the data on yen *appreciations* was drawn from a process with infinite second moment, rather than Merton's compound Poisson normal process.

Table 6 [about here]

Table 6 shows exponentially dampened power-law parameter estimates for positive (yen *depreciation*) jumps. Once again a compound Poisson jump process is rejected in favor of a model that yields a power-law tail. However, in contrast to negative jumps, the positive jump data for $\alpha = 0.01$ favors a pure power-law (Pareto) distribution in the tail rather than exponentially dampened power-law as indicated by log likelihood and AIC values. Moreover, the power exponent $\zeta = 3.2$ indicates a regime closer to Gaussian, with a finite second moment rather than a Levy process, as was found for yen *appreciation* jumps. The difference in parameter estimates and in their behavior across jumps of different significance levels indicate that while both negative and positive jumps follow distributions with power-law tails, the underlying data generating processes are not the same. This is confirmed by the simulations of $\alpha = 0.05$ jumps shown in Figure 6, with the exponentially dampened power-law parameters from Tables 5 and 6.

Figure 6 [about here]

The top panel in Figure 6 corresponds to the simulated series, while the bottom panel displays the empirical observations of jumps. The amplitude in fluctuations is higher for both empirical and simulated series for the negative jumps. The simulation of the negative jump series matches the pattern of the data in generating small jump periods punctuated by extreme deviations. This is not the case for the positive jumps. The simulation based on distribution parameter estimates of positive jumps produces a series more even in magnitude, consistent with the lower variability of the observed positive jumps. Based on simulation results, we suspect that the underlying data generating process differs for negative and positive jumps, with negative jumps subject to more extreme fluctuations. The contrast between the simulation results of yen appreciation (negative) and yen depreciation (positive) jumps clearly captures the origins of the negative skewness of JPY/USD returns.

Finally, the model predicts the power exponent of 1.5 in the exponentially dampened power-law. Our empirical estimates for the exponent, conditional on the cut-off value for the tail selected based on the best fit for the Pareto distribution have yielded estimates of the exponent in the neighborhood of 2. This gap may be rectified by modifications on estimation and modeling. Table 7 illustrates that under an alternative selection criteria for the cut-off, κ_{min}, estimates of 1.5 for ζ are also within the feasible range. The lower cut-off on the tail observations has been selected as one standard deviation in the empirical jump data. Under this more inclusive specification the power-law exponent is 1.527 for negative jumps and 1.495 for positive jumps.

Table 7 [about here]

Alternatively, it is known that the power exponent ζ derived in the model is increased above 1.5 if the parameter μ is taken gradually from below the criticality $\mu < 1$ toward the criticality during the time span of observations. This mechanism is called a "sweeping" of control parameter towards a critical point (Sornette (2006)). Recall the case in which we repeat the static equilibrium over periods where the currency position k is updated over the periods. When k is small, the tatonnement is likely to be subcritical, with $\mu < 1$, while μ is increased toward 1 as k increases. Thus, the effect of possible sudden yen *appreciation* due to the collective unwinding becomes more significant on the overall return when the volume of existing carry trade position is large. If our data is generated by such a process, the situation exactly falls in the scenario of the sweeping of a parameter where the key parameter μ gradually sweeps toward the criticality at 1. In this case, the observed jumps exhibit dampened power-law with exponent greater than 1.5. The exact value of the exponent depends on how the parameter μ is increased over periods.

5.7 Economic Determinants of the "Tail Risk"

The model imposes a number of restrictions on the relationship between $\phi = \mu - 1 - log(\mu)$ and the economic variables related to carry trade activity. We begin with a subsample analysis. Since the stochastic dynamics in carry trade are conditional on non-negligible positive carry, δ, we expect the distribution parameters to take on model-implied values when the interest rate differential between U.S. and Japan was relatively sizable. Table 8 shows distribution parameter estimates for subsamples of high and low interest rate differentials considered in the previous sub-section. The

power exponent, ζ, for yen appreciation jumps is 2.007 when the differential is high (closer to 1.5 implied by the model) compared to 2.394 when the differential is low. The exponential truncation parameter ϕ is 1.250 when the interest differential is high compared to 1.410 when the differential is low. For both parameters the difference is approximately 2 standard deviations, significant at the 5 percent level. The lower ϕ during higher interest rate differential period indicates the exponential truncation point further in the tail of the distribution – a higher "tail risk." Intuitively, this means that when the interest differential is high a larger adjustment is induced by the same size pertrubation, that is a larger number of traders, m, would have unwound their carry positions having observed an "independent" uniwinding action of an initial trader $m_0 = 1$.

In addition to the interest rate differential we also split the sample by VIX. Although a risk-neutral setup is sufficient to generate the necessary dynamics, we expect higher risk aversion (also to the extent that it is associated with tighter funding constraints) to be associated with higher "tail risk" (lower ϕ). Table 9 shows distribution parameter estimates for subsamples split by the level of VIX. Consistent with the above hypothesis, when VIX is high then the exponentially dampened power-law has a higher log likelihood than a simple Pareto. We also get a considerably lower estimate of ϕ compared to when VIX is low, 0.620 versus 3.327, with the difference significant at 1 percent level.

Tables 8 & 9 [about here]

Figure 7 shows the kernel density plots of yen *appreciation* jumps for high and low VIX subsamples analyized in Table 9. The figure confirms that lower ϕ during high VIX periods is associated with a more stretched tail of the distribution. Thus, risk in the JPY/USD currency market appears to be directly linked to risk aversion and uncertainty in broader financial markets.

Figure 7 [about here]

The extreme case of $\phi = 0$ corresponds to the criticality of $\mu = 1$. Then, the model generates a pure power-law distribution for m and the branching process becomes a martingale, that is the conditional expectation then is that all managers liquidate next period if all are liquidating in the current period. At this stage, the feedback between traders is at a maximum and will eventually lead all traders to coordinate on the same action. The top panel of Figure 8 shows data simulated using

a power-law fit to the negative jump series. The simulation approximates the general amplitude in the fluctuations of the empirical data shown in the bottom panel except for the one "catastrophic" event when the simulated jump exceeds 11 in absolute value. The simulation illustrates the ability of the model to incorporate "rare" disasters and day-to-day volatility in the same data generating process. This is because the estimates of the power exponent (tail index) for yen *appreciation* jumps favor a Levy regime with undefined second moment entailing the probability of an "extreme" event much higher than can be drawn from a Gaussian regime.

Figure 8 [about here]

The preceding analysis has shown that the crash risk of the carry currency rises exponentially as $\phi \to 0$. In order to better understand the economic determinants of such "tail risk", we conduct a structural examination of the dependence of ϕ on the variables related to carry trade based on Equation (18). Equation (18) allows us to sign the impact of accumulated carry positions, k, expected "crash," $(\Delta s_H - \Delta s_L)$, and margin requirements, M, on ϕ. The second column of Table 10 lists the expected signs of the impact on ϕ, based on partial differentiation of μ with respect to each variable; recall that a higher intensity in the branching process μ implies exponential truncation further in the tail of the distribution hence lower ϕ. The fourth column of Table 10 lists the empirical proxies for k, $(\Delta s_H - \Delta s_L)$, and M respectively. We proxy for k with CME non-commercial short futures positions in the yen (which CFTC classifies as speculative), for $(\Delta s_H - \Delta s_L)$ we proxy with the values of risk reversals, and for M we use historical margin requirement data for yen futures trading obtained from the CME group[15] We use initial margin requirement data on speculative positions. In addition, we also control for risk aversion, denoted as ρ, using historical VIX. We do this for two reasons: first, to the extent that VIX proxies not only for risk aversion but also for funding conditions, it is an important variable for gaging speculative forces in foreign exchange, and second, since the value of risk reversals conveys option implied skewness *and* skewness risk premium, or equivalently $(\Delta s_H - \Delta s_L)\rho$, it is necessary to control for risk aversion separately with

[15]CME Group sets four margin requirements for currency futures, namely initial and maintenance margins on speculators and hedgers/members. A sample margin requirement report is shown in Figure 13. A trader is classified as a "speculator" if the trader is not identified as hedging a foreign exchange exposure according to the entity's Statement of Reporting Trader (CFTC Form 40). The CFTC staff may re-classify the trader if they possess additional information about the trader's use of the futures market. The "speculator" or "non-commercial" category mostly includes professional money managers such as hedge funds and commodity trading advisers. A sample report if shown in Figure 14. For further details see http://www.cftc.gov/MarketReports/CommitmentsofTraders/.

a proxy such as the VIX. While we were able to obtain data on non-commercial shorts and the VIX and CME initial speculative margin requirement in yen futures for the entire January 1, 1999 through February 1, 2007 period, the risk reversal data was only available as of September 2003.

Table 10 [about here]

Again, we use Bayesian econometrics, which provide convenient tools for treating distribution parameters themselves as stochastic. We use Bayesian MCMC implemented via Metropolis-Hastings (MH) method.[16][17] It is more parsimonious than Gibbs sampling in that it does not require a conjugate prior for each distribution parameter, but samples from a proportional probability distribution to the density to be calculated. We use an MH algorithm to sample from the following hierarchical model:

$$Pr(\kappa_j) \propto \kappa_j^{-1.5} e^{-\phi_j \kappa_j}, \text{ and} \tag{22}$$

$$\phi_j = \gamma_0 + \sum_{l=1}^{4} \gamma_{l,j} X_{l,j} + \epsilon_j;\ j = 1, 2 \ldots, J, \tag{23}$$

with priors,

$$\gamma_0 \sim N(\mu_0, \sigma_0), \tag{24}$$

$$\gamma_l \sim N(\mu_l, \sigma_l), \text{ and} \tag{25}$$

$$\tau_\epsilon \sim \Gamma(\alpha_\epsilon, \beta_\epsilon) \tag{26}$$

where $N(\cdot)$ and $\Gamma(\cdot)$ denote Normal and Gamma distributions. The hyper-parameters for γ_0 and γ_l's were selected such that prior means match the MLE estimates. We account for additional variability in ϕ via a random effects term, ϵ_j, whose precision is measured by τ_ϵ. We are most interested in obtaining the coefficient vector of γ_l's on the vector of four controls, $\mathbf{X} = [k,\ \rho,\ M,\ (\Delta s_H - \Delta s_L)]$: the volume of non-commercial yen short futures, VIX, the CME margin requirement, and risk reversals. The first three values are nominal, and therefore enter

[16]The estimation was conducted with WinBUGS software following the Bayesian modeling framework outlined in Lunn et al. (2000).

[17]See Chib and Greenberg (1995) for a comprehensive reference on Metropolis-Hastings algorithm.

in logs. The risk reversals enter with a 1 day lag in order to avoid endogeneity issues due to the posssible reverse causality from a yen appreciation jump to higher absolute value of risk reversals.

Table 11 [about here]

Table 11 shows the estimation results. The signs of the coefficients are consistent with model hypothesis: higher k and $(\Delta s_H - \Delta s_L)$ are associated with an increased "tail risk" of sharp yen appreciation (lower ϕ), while higher M is associated with lower risk (higher ϕ). The coefficients on non-commercial speculative short yen positions, k, are statistically significant under all specifications confirming our main hypothesis that carry trade plays a major role in stochastic volatility of the JPY/USD exchange rate. The coefficient on VIX is also negative indicating that higher VIX is associated with a more elongated tail on the yen appreciation side (or equivalently more negative skewness in JPY/USD as found in Brunnermeier et al. (2009)), but becomes insignificant when controlling for speculative short positions. This indicates that risk aversion and funding considerations implicit in the value of VIX affect the skewness of the JPY/USD exchange rate primarily through changes in carry trader positions, k.

The coefficients on margin requirement and risk reversals, although of the hypothesized sign, are insignificant when added sequentially. For instance, the coefficient on M in specification (5) is 1.024 (standard error 0.719) indicating that M has statistically significant positive impact on ϕ at the 68% but not at the 95% confidence level. This may be due to much lower variability in the margin requirement which changed anywhere between 3 to 10 times per year during our sample period. Shorter sample in the case of risk reversals is another impediment. When we restrict the vector of controls of ϕ to a constant, lagged risk reversals, and random effect, then the coefficient on risk reversals more than doubles, and is statistically significant at 5 percent level.[18]

Figure 9 [about here]

[18]The inference of coefficient significance and correlations rest on the assumption of unbiasedness of the estimates. Figure 11 shows Bayesian MCMC diagnostic plots for γ_1 through γ_4. The first column plots the density of the samples. Symmetric bell curves indicate a good mixture and that a normal approximation to the standard errors is reasonable. The second column plots the rapidly declining autocorrelation function of the samples indicating a rapid mixing with estimates theselves approaching white noise. The third column shows a visual test for endogeneity via a scatter plot between sampled slope coefficients and the random effects component, τ_ϵ, which is bounded at zero from below. The scatter plots show a random spread consistent with exogeneity of the controls. Finally, Figure 12 shows Metropolis acceptance rates with acceptance rates reaching the stationary level around the commonly accepted level of 0.234 random walk MH algorythm within 1,000 to 2,000 samples; we discard the first 4,000 using the subsequent 10,000 for inference.

Figure 9 shows the pairwise scatter plot of the sampled coefficients, where γ_1, γ_2, γ_3, and γ_4 are coefficients on CME speculative positions, VIX, CME margin requirement, and risk reversals respectively. While most scatter plots show a random spread (no multicollinearity) the scatter plot between γ_1 and γ_3 (γ_1 and γ_4) exhibit a negative (positive) correlation. Figure 10 shows the blowup plots for these coefficient pairs with best linear fit. The correlation between coefficients on speculative positions and margin requirement (γ_1 and γ_3) is -0.3528, and the correlation between coefficients on speculative positions and risk reversals (γ_1 and γ_4) is 0.1650, with $p-value$=0.0000 for both. Such complementarity between the effect of k, M, and $(\Delta s_H - \Delta s_L)$ has a ready economic interpretation based on Equation (18). Recall that both M^{-1} and $(\Delta s_H - \Delta s_L)$ affect the intensity of the chain reaction in carry unwinding multiplicatively with k. This indicates that tougher margin requirements have an effect of reducing the probability of extreme yen appreciation by mitigating the impact of carry trade activity. Similarly, expectations of sharp yen appreciation tend to be self-fulfilling and further increase the probability of extreme yen appreciation through the actions of carry traders.

To summarize, this subsection served the dual purpose of testing the implications of the model and identifying the sources of "tail risk" for rare but significant events of a sharp yen appreciation. The findings point at carry trade as the major factor. First, stochastic volatility on the yen appreciation side is more extreme when the incentive for currency speculation is higher (higher δ); second, stochastic volatility on the yen appreciation side is positively associated with a greater volume of speculative positions (proxied by CME non-commercial short yen futures contracts); and third, the effects of other financial variables, such as the VIX, margin requirement, and option implied expectations of yen appreciation risk appear to affect the probability of extreme yen appreciation through the carry trade channel.

6 Conclusion

This paper indetifies and empirically tests several features of speculative dynamics that contribute to such stylized facts as skewness and excess volatility in foreign exchange returns, otherwise known as the *exchange rate disconnect puzzle* . We model strategic traders trying to profit from the interest rate differential between two countries at the expense of exposing themselves to currency

crash risk. The common uncertainty about the "day of reckoning" makes it rational for carry traders to infer information from each others' trades. This introduces an element of dependency in traders' actions leading to endogenous episodes of "explosive" carry unwinding via a chain reaction through information revelation. While the underlying dynamics are generated by the propensity of carry traders to herd, leverage can exacerbate the chain reaction in carry unwinding. The impact of leverage is highly non-linear, and suggests that there may exist an optimal percentage margin requirement on speculative positions which is a function of the interest rate differential between high and low yielding currencies.

In equilibrium, the distribution of the number of traders unwinding their positions fluctuates according to a power-law with exponential truncation, and with a linear price impact function, so too do the jumps in foreign exchange returns. The model yields a power-law exponent of -1.5 in the density function of jumps, which is found to be in the feasible range of our empirical estimates from the JPY/USD exchange rate.

Because of prolonged "zero interest rate" policy of the Bank of Japan, the Japanese yen in particular has served as a funding currency in carry trade. Consistent with day to day volatility dynamics being influenced by carry trade, only yen appreciation jumps exhibit dependence and follow a Levy regime with unbounded variation, while yen depreciation jumps are best described as white noise. In particular, we find that sharp yen appreciations over the period from January 1, 1999 through February 1, 2007 are more likely to follow an exponentially dampened power-law than Merton's compound Poisson normal process. The asymmetries and higher negative skew of JPY/USD returns are confirmed by simulations based on estimated distribution parameters. Since only yen appreciations would have been costly to carry traders producing different dynamics on the way up than on the way down, such asymmetries are consistent with the role of the yen as a funding currency in carry trade during our sample period.

Based on parametric restrictions from the model we identify economic factors that lead to extreme volatility by intensifying the herd effect. In the analysis of subsamples we find that the key distribution parameter that captures the intensity of herding is higher during times of greater interest rate differential and higher values of VIX. Fitting the model in reduced form to the data, we find that tougher margin requirements have an effect of reducing the probability of extreme yen appreciation by mitigating the impact of carry trade activity. Similarly, expectations

of sharp yen appreciation tend to be self-fulfilling and further increase the probability of extreme yen appreciation through the actions of carry traders. The impact of the volume of speculative futures on the "tail risk" is particularly robust, corroborating the key hypothesis that speculative dynamics play a destabilizing role in foreign exchange markets.

Our data do not include "extreme" episodes in JPY/USD return volatility corresponding to the 1998 LTCM collapse and the 2008 sub-prime crisis. Yet, exponentially dampened power-law parameter estimates indicate that the data comes from a distribution that generates yen *appreciation* jumps with unbounded variation, essentially attributing rare market crashes and normal return volatility to the same underlying mechanism.

References

Abreu, D. and Brunnermeier, M. (2003), "Bubbles and crashes", *Econometrica* , Vol. 71, pp. 173–204.

Abreu, D. and Brunnermeier, M. K. (2002), "Synchronization risk and delayed arbitrage", *Journal of Financial Economics* , Vol. 66, pp. 341–360.

Alfarano, S., Lux, T. and Wagner, F. (2005), "Estimation of agent-based models: The case of an asymmetric herding model", *Computational Economics* , Vol. 26, pp. 19–49.

Alfarano, S., Lux, T. and Wagner, F. (2008), "Time variation of higher moments in a financial market with heterogeneous agents: An analytical approach", *Journal of Economic Dynamics and Control* , Vol. 32, pp. 101–136.

Andersen, T. G., Bollerslev, T. and Diebold, F. X. (2007), "Roughing it up: Including jump components in the measurement, modeling, and forecasting of return volatility", *The Review of Economics and Statistics* , Vol. 89, pp. 701–720.

Arnold, B. C. and Press, S. J. (1983), "Bayesian inference for pareto populations", *Journal of Econometrics* , Vol. 21, pp. 287 – 306.

Avery, C. and Zemsky, P. (1998), "Multidimensional uncertainty and herd behavior in financial markets", *American Economic Review* , Vol. 88, pp. 724–48.

Bakshi, G., Carr, P. and Wu, L. (2008), "Stochastic risk premiums, stochastic skewness in currency options, and stochastic discount factors in international economies", *Journal of Financial Economics* , Vol. 87, pp. 132–156.

Banerjee, A. V. (1992), "A simple model of herd behavior", *The Quarterly Journal of Economics* , Vol. 107, pp. 797–817.

Barndorff-Nielsen, O. E. (2004), "Power and bipower variation with stochastic volatility and jumps", *Journal of Financial Econometrics* , Vol. 2, pp. 1–37.

Barndorff-Nielsen, O. E., Graversen, S. E., Jacod, J. and Shephard, N. (2006), "Limit theorems for bipower variation in financial econometrics", *Econometric Theory* , Vol. 22, pp. 677–719.

Barndorff-Nielsen, O. E. and Shephard, N. (2006), "Econometrics of testing for jumps in financial economics using bipower variation", *Journal of Financial Econometrics* , Vol. 4, pp. 1–30.

Bass, R. F. and Burdzy, K. (1999), "Stochastic bifurcation models", *Annals of Probability* , Vol. 27, pp. 50–108.

Beine, M., Lahaye, J., Laurent, S., Neely, C. J. and Palm, F. C. (2007), "Central bank intervention and exchange rate volatility, its continuous and jump components", *International Journal of Finance & Economics* , Vol. 12, pp. 201–223.

Bikhchandani, S., Hirshleifer, D. and Welch, I. (1992), "A theory of fads, fashion, custom, and cultural change in informational cascades", *Journal of Political Economy* , Vol. 100, pp. 992–1026.

Brock, W. A., Scheinkman, J. A., Dechert, W. D. and LeBaron, B. (1996), "A test for independence based on the correlation dimension", *Econometric Reviews* , Vol. 15, pp. 197–235.

Brunnermeier, M. K., Nagel, S. and Pedersen, L. H. (2009), "Carry trades and currency crashes", *NBER Macroeconomics Annual* , Vol. 23, pp. 313–348.

Burnside, A. C., Eichenbaum, M. S., Kleshchelski, I. and Rebelo, S. (2008), Do peso problems explain the returns to the carry trade?, NBER Working Papers 14054, National Bureau of Economic Research, Inc.

Burnside, C., Eichenbaum, M. and Rebelo, S. (2007), "The returns to currency speculation in emerging markets", *American Economic Review* , Vol. 97, pp. 333–338.

Candelon, B. and Straetmans, S. (2006), "Testing for multiple regimes in the tail behavior of emerging currency returns", *Journal of International Money and Finance* , Vol. 25, pp. 1187–1205.

Cecchetti, S. G., Fender, I. and McGuire, P. M. (2010), Toward a global risk map, BIS Working Paper Series 309, Bank for International Settlements.

Chari, V. V. and Kehoe, P. J. (2004), "Financial crises as herds: overturning the critiques", *Journal of Economic Theory* , Vol. 119, pp. 128–150.

Chib, S. and Greenberg, E. (1995), "Understanding the metropolis-hastings algorithm", *The American Statistician* , Vol. 49, pp. 327–335.

Clauset, A., Shalizi, C. R. and Newman, M. E. J. (2009), "Power-law distributions in empirical data", *SIAM Review* , Vol. 51, p. 661.

Duffie, D., Grleanu, N. and Pedersen, L. H. (2002), "Securities lending, shorting, and pricing", *Journal of Financial Economics* , Vol. 66, pp. 307 – 339.

Engel, C. (1996), "The forward discount anomaly and the risk premium: A survey of recent evidence", *Journal of Empirical Finance* , Vol. 3, pp. 123–192.

Farhi, E., Fraiberger, S. P., Gabaix, X., Ranciere, R. and Verdelhan, A. (2009), Crash risk in currency markets, NBER Working Papers 15062, National Bureau of Economic Research, Inc.

Farhi, E. and Gabaix, X. (2008), Rare disasters and exchange rates, NBER Working Papers 13805, National Bureau of Economic Research, Inc.

Flood, R. P. and Rose, A. K. (1993), Fixing exchange rates: A virtual quest for fundamentals, NBER Working Papers 4503, National Bureau of Economic Research, Inc.

Gagnon, J. E. and Chaboud, A. P. (2007), What can the data tell us about carry trades in japanese yen?, International Finance Discussion Papers 899, Board of Governors of the Federal Reserve System.

Galati, G., Heath, A. and McGuire, P. (2007), "Evidence of carry trade activity", *BIS Quarterly Review* .

Galati, G., Higgins, P., Humpage, O. and Melick, W. (2007), "Option prices, exchange market intervention, and the higher moment expectations channel: a user's guide", *International Journal of Finance & Economics* , Vol. 12, pp. 225–247.

Gul, F. and Lundholm, R. (1995), "Endogenous timing and the clustering of agents' decisions", *Journal of Political Economy* , Vol. 103, pp. 1039–66.

Hansen, L. P. and Hodrick, R. J. (1980), "Forward exchange rates as optimal predictors of future spot rates: An econometric analysis", *Journal of Political Economy* , Vol. 88, pp. 829–53.

Harris, T. E. (1989), *The Theory of Branching Processes*, Dover, NY.

Hochradl, M. and Wagner, C. (2010), "Trading the forward bias: Are there limits to speculation?", *Journal of International Money and Finance* , Vol. 29, pp. 423 – 441.

Hsieh, D. A. (1989), "Testing for nonlinear dependence in daily foreign exchange rates", *The Journal of Business* , Vol. 62, The University of Chicago Press, pp. 339–368.

Hutchison, M. M. and Sushko, V. Y. (2010), Impact of macroeconomic surprises on carry trade activity, Working Paper Series 10-10, Santa Cruz Institute for International Economics.

Ichiue, H. and Koyama, K. (2008), Regime switches in exchange rate volatility and uncovered interest rate parity, Working paper series, Bank of Japan.

Jansen, D. W. and de Vries, C. G. (1991), "On the frequency of large stock returns: Putting booms and busts into perspective", *The Review of Economics and Statistics* , Vol. 73, pp. 18–24.

Kirman, A. (1993), "Ants, rationality, and recruitment", *The Quarterly Journal of Economics* , Vol. 108, pp. 137–56.

Klitgaard, T. and Weir, L. (2004), "Exchange rate changes and net positions of speculators in the futures market", *Economic Policy Review* , pp. 17–28.

Longin, F. M. (1996), "The asymptotic distribution of extreme stock market returns", *Journal of Business* , Vol. 69, pp. 383–408.

Lunn, D., Thomas, A., Best, N. and Spiegelhalter, D. (2000), "Winbugs - a bayesian modelling framework: concepts, structure, and extensibility.", *Statistics and Computing* , Vol. 10, pp. 325–337.

Morris, S. and Shin, H. (1998), "Unique equilibrium in a model of self-fulfilling currency attacks", *American Economic Review* , Vol. 88, p. 587597.

Morris, S. and Shin, H. S. (1999), "Risk management with interdependent choice", *Oxford Review of Economic Policy* , Vol. 15, pp. 52–62.

Mussa, M. (1986), "Nominal exchange rate regimes and the behavior of real exchange rates: Evidence and implications", *Carnegie-Rochester Conference Series on Public Policy* , Vol. 25, pp. 117–214.

Nirei, M. (2006), "Threshold behavior and aggregate fluctuation", *Journal of Economic Theory* , Vol. 127, pp. 309–322.

Nirei, M. (2008), "Self-organized criticality in a herd behavior model of financial markets", *Journal of Economic Interaction and Coordination* , Vol. 3, pp. 89–97.

Nirei, M. and Sushko, V. (2010), Stochastic herding by institutional investment managers, Working Papers 64, Hitotsubashi University, Research Center for Price Dynamics.

Plantin, G. and Shin, H. S. (2010), Carry trades and speculative dynamics, Working papers, Toulouse School of Economics and Princeton University.

Quintos, C., Fan, Z. and Phillips, P. C. B. (2001), "Structural change tests in tail behaviour and the asian crisis", *Review of Economic Studies* , Vol. 68, pp. 633–63.

Rajan, R. G. (2006), "Has finance made the world riskier?", *European Financial Management* , Vol. 12, pp. 499–533.

Scharfstein, D. S. and Stein, J. C. (1990), "Herd behavior and investment", *American Economic Review* , Vol. 80, pp. 465–79.

Sornette, D. (2006), *Critical Phenomena in Natural Sciences*, second edn, Springer.

Vives, X. (2008), *Information and Learning in Markets*, Princeton University Press.

Wu, L. (2006), "Dampened power law: reconciling the tail behavior of financial security returns", *Journal of Business* , Vol. 78, pp. 1445–1473.

A Proof of Proposition 1

By taking a partial derivative with respect to m for a fixed $\bar{x}$, we have:

$$\frac{\partial}{\partial m}\log\frac{\Pr(\text{High} \mid x_i=\bar{x},m)}{\Pr(\text{Low} \mid x_i=\bar{x},m)} = \log\frac{F(\bar{x})}{G(\bar{x})}-\log\frac{1-F(\bar{x})}{1-G(\bar{x})} \tag{A.1}$$

$$< 0 \tag{A.2}$$

where the inequality obtains because of $F/G < f/g < (1-F)/(1-G)$ since f/g is increasing. Thanks to the MLRP, we also have the following properties:

$$\frac{\partial}{\partial \bar{x}}\log\frac{f(\bar{x})}{g(\bar{x})} > 0 \tag{A.3}$$

$$\frac{\partial}{\partial \bar{x}}\log\frac{F(\bar{x})}{G(\bar{x})} = \frac{g(\bar{x})}{F(\bar{x})}\left(\frac{f(\bar{x})}{g(\bar{x})}-\frac{F(\bar{x})}{G(\bar{x})}\right)>0 \tag{A.4}$$

$$\frac{\partial}{\partial \bar{x}}\log\frac{1-F(\bar{x})}{1-G(\bar{x})} = -\frac{g(\bar{x})}{1-F(\bar{x})}\left(\frac{f(\bar{x})}{g(\bar{x})}-\frac{1-F(\bar{x})}{1-G(\bar{x})}\right)>0 \tag{A.5}$$

Then, the partial derivative of the left-hand side of (3) with respect to $\bar{x}$ becomes:

$$\frac{\partial}{\partial \bar{x}}\log\frac{\Pr(\text{High} \mid x_i=\bar{x},m)}{\Pr(\text{Low} \mid x_i=\bar{x},m)} = \frac{\partial}{\partial \bar{x}}\log\frac{f(\bar{x})}{g(\bar{x})}+m\frac{\partial}{\partial \bar{x}}\log\frac{F(\bar{x})}{G(\bar{x})}+(N-1-m)\frac{\partial}{\partial \bar{x}}\log\frac{1-F(\bar{x})}{1-G(\bar{x})} \tag{A.6}$$

$$> 0 \tag{A.7}$$

The partial derivative of the right-hand side of (3) is:

$$\frac{\partial}{\partial m}\log\frac{-\Delta s_L-\delta}{\Delta s_H+\delta} = \frac{(\Delta s_L-\Delta s_H)(k-1)\Delta s'}{-(\Delta s_H+\delta)(\Delta s_L+\delta)} \tag{A.8}$$

$$> 0 \tag{A.9}$$

Collecting terms, we obtain:

$$\frac{d\bar{x}}{dm} = \frac{-\log\frac{F(\bar{x})}{G(\bar{x})}+\log\frac{1-F(\bar{x})}{1-G(\bar{x})}+\frac{(\Delta s_L-\Delta s_H)(k-1)\Delta s'}{-(\Delta s_H+\delta)(\Delta s_L+\delta)}}{\frac{\partial}{\partial \bar{x}}\log\frac{f(\bar{x})}{g(\bar{x})}+m\frac{\partial}{\partial \bar{x}}\log\frac{F(\bar{x})}{G(\bar{x})}+(N-1-m)\frac{\partial}{\partial \bar{x}}\log\frac{1-F(\bar{x})}{1-G(\bar{x})}} \tag{A.10}$$

$$= \frac{-\log\frac{F(\bar{x})}{G(\bar{x})}+\log\frac{1-F(\bar{x})}{1-G(\bar{x})}+\frac{(\Delta s_L-\Delta s_H)(k-1)\Delta s'}{-(\Delta s_H+\delta)(\Delta s_L+\delta)}}{\frac{f'(\bar{x})-g'(\bar{x})}{f(\bar{x})/g(\bar{x})}+m\left(\frac{f(\bar{x})}{F(\bar{x}))}-\frac{g(\bar{x})}{G(\bar{x})}\right)+(N-1-m)\left(\frac{g(\bar{x})}{1-G(\bar{x})}-\frac{f(\bar{x})}{1-F(\bar{x})}\right)} \tag{A.11}$$

which is strictly positive by the inequalities shown above.

B Empirical Methodology

B.1 Jump component

In the limit (as $\Delta \to 0$) realized daily volatility approaches the continuously aggregated sum of square returns:

$$RV_{t+1}(\Delta) \to \int_t^{t+1}\sigma^2(s)ds+\sum_{t<s\le t+1}\kappa^2(s) \tag{B.1}$$

and $BV_t(\Delta)$ is defined as the sum of the product of adjacent absolute intraday returns standardized by a constant:

$$BV_t(\Delta) \equiv \mu^{-2} \sum_{j=2}^{1/\Delta} |r_{t+j\Delta,\Delta}||r_{t+(j-1)\Delta,\Delta}| \tag{B.2}$$

where $\mu \equiv (2/\pi)^2$ is the mean of the absolute value of standard normally distributed random variable. Since returns from two adjacent time periods share the persistent volatility but not the sporadic jumps, it follows from (B.2) that bi-power variation provides a reasonable proxy for the persistent component of the volatility. Barndorff-Nielsen et al. (2006) show that:

$$BV_{t+1}(\Delta) \to \int_t^{t+1} \sigma^2(s)ds \tag{B.3}$$

as $\Delta \to 0$.

Since realized volatility, $RV_{t+1}(\Delta)$, and bi-power volatility, $BV_{t+1}(\Delta)$, can be directly calculated from the observed asset prices, it follows that the jump component can be approximated as the difference of the two:

$$RV_{t+1}(\Delta) - BV_{t+1}(\Delta) \to \sum_{t<s\leq t+1} \kappa^2(s) \tag{B.4}$$

Because of a finite sample the estimate of the squared jump process might be negative so Beine et al. (2007) truncate the measurement at zero to get:

$$\kappa_{t+1}(\Delta) \equiv max[RV_{t+1}(\Delta) - BV_{t+1}(\Delta), 0] \tag{B.5}$$

We select only significant jumps while discounting smaller jumps as a part of continuous process or noise. Andersen et al. (2007) derive an asymptotically standard-normally distributed test statistic based on the fourth moment of the jump-diffusion process:

$$Z_{t+1}(\Delta) \equiv \Delta^{1/2} \frac{[RV_{t+1}(\Delta) - BV_{t+1}(\Delta)]RV_{t+1}(\Delta)^{-1}}{[(\mu^4 + 2\mu^2 - 5)max\{1, TQ_{t+1}(\Delta)BV_{t+1}(\Delta)^{-2}\}]^{1/2}} \tag{B.6}$$

where,

$$TQ_{t+1}(\Delta) \equiv \Delta^{-1}\nu^{-3} \sum_{j=3}^{1/\Delta} |r_{t+j\Delta,\Delta}|^{4/3}|r_{t+(j-1)\Delta,\Delta}|^{4/3}|r_{t+(j-2)\Delta,\Delta}|^{4/3} \tag{B.7}$$

$$\nu \equiv 2^{2/3}\Gamma(7/6)\Gamma(1/2)^{-1} \tag{B.8}$$

so that $TQ_{t+1}(\Delta) \to \int_t^{t+1} \sigma^4(s)ds$ as $\Delta \to 0$.

Hence, choosing to estimate fewer but larger jumps amounts to choosing a smaller significance level α associated with critical value Φ_α to compute:

$$\kappa_{t+1,\alpha}(\Delta) = I[Z_{t+1}(\Delta) > \Phi_\alpha] \cdot [RV_{t+1}(\Delta) - BV_{t+1}(\Delta)] \tag{B.9}$$

In addition to reporting all jumps, we report jumps estimated with $\alpha = 0.05$ and $\alpha = 0.01$. As a final step of implementing (B.9) Andersen et al. (2007) tackle first order autocorrelation due to microstructure noise by dividing $BV_{t+1}(\Delta)$ and $TQ_{t+1}(\Delta)$ by $(1 - 2\Delta)$ and $(1 - 4\Delta)$ respectively and adjusting the lags on returns.

B.2 Bayesian Markov Chain - Monte Carlo (MCMC) Estimation of ζ and ϕ

Under the assumption of exponentially dampened power-law for $\kappa_j \geq \kappa_{min}$ using equation (5.6) the joint likelihood is:

$$f(\kappa_1, \kappa_2, .., \kappa_J) \propto \prod_{j=1}^{J} \kappa_j^{-\zeta} exp\{-\phi\kappa_j\} \tag{B.10}$$

The conjugate prior families for the power exponent and exponential decay parameter are Gamma families[19]: $\zeta \sim$ Gamma (α_ζ, β_ζ) and $\phi \sim$ Gamma (α_ϕ, β_ϕ). Combining prior parameter densities with equation (B.10) and assuming ζ and ϕ are orthogonal we obtain the joint posterior:

$$f(\zeta, \phi|\kappa_1, \kappa_2, .., \kappa_J) \propto \left[\prod_{j=1}^{J} \kappa_j^{-\zeta}\right] \zeta^{\alpha_\zeta - 1} exp\{-\beta_\zeta\zeta\} \left[exp\left\{-(\sum_{j=1}^{J} \kappa_j + \beta_\phi)\phi\right\}\right] \phi^{\alpha_\phi - 1} \tag{B.11}$$

From (B.11) we obtain complete parameter conditionals:

$$f(\zeta|\kappa_1, \kappa_2, .., \kappa_J) \propto \zeta^{\alpha_\zeta - 1} exp\left\{-(\beta_\zeta + \sum_{j=1}^{J} ln(\kappa_j))\zeta\right\} \tag{B.12}$$

and

$$f(\phi|\kappa_1, \kappa_2, .., \kappa_J) \propto \phi^{\alpha_\phi - 1} exp\left\{-(\beta_\phi + \sum_{j=1}^{J} \kappa_j)\phi\right\} \tag{B.13}$$

From (B.12) and (B.13)it follows that we can apply the Gibbs step in the MCMC algorithm to sample the power exponent and the exponential decay parameter from the following distributions respectively:

$$\zeta|\kappa_1, \kappa_2, .., \kappa_J \sim \text{Gamma } (\alpha_\zeta, \beta_\zeta + \textstyle\sum_{j=1}^{J} ln(\kappa_j)) \tag{B.14}$$

$$\phi|\kappa_1, \kappa_2, .., \kappa_J \sim \text{Gamma } (\alpha_\phi, \beta_\phi + J\bar{\kappa}) \tag{B.15}$$

For each jump sample we have a strong prior for the parameters based on preliminary MLE results, therefore we chose prior parameters such that $\alpha_\zeta/\beta_\zeta = \hat{\zeta}_{MLE}$ and $\alpha_\phi/\beta_\phi = \hat{\phi}_{MLE}$.

[19] See Arnold and Press (1983) for the detailed discussion on the Bayesian techniques to estimate parameters in the power-law distribution

C Tables and Figures

Table 1: **Expectations of a large yen appreciation and carry trade positions.**The table shows Granger-causality test between risk reversals and net non-commercial yen short futures positions on CME, a common proxy for carry trade.

	Baseline				Controlling for exchange rate			
	1-lag		2-lag		1-lag		2-lag	
	RRs cause NCMS	NCMS cause RRs	RRs cause NCMS	NCMS cause RRs	RRs cause NCMS	NCMS cause RRs	RRs cause NCMS	NCMS cause RRs
1-Month Risk Reversals								
F-Statistic	3.837**	0.483	8.832***	2.213	4.326**	0.362	8.374***	1.409
Probability	0.052	0.488	0.000	0.113	0.039	0.548	0.000	0.248
Coeff. Sum	6.042	0.002	21.439	0.000	7.683	0.002	24.116	0.004
Obs.	146		143		146		143	
1-Year Risk Reversals								
F-Statistic	9.023***	0.521	9.611***	2.570*	7.720***	0.022	6.924***	1.798
Probability	0.003	0.471	0.000	0.080	0.006	0.882	0.001	0.169
Coeff. Sum	14.491	0.001	29.964	-0.003	15.495	0.000	30.388	-0.005
Obs.	151		150		151		150	

Note: *, **, and *** indicate the null hypothesis of no Granger-causality is rejected with significance levels of 10%, 5%, and 1% respectively. Risk reversals are options contracts used to hedge against the risk of substantial unidirectional price movement, and as such their values are often treated as a proxy for market expectations about sharp yen appreciation. The value of risk reversal equals the implied volatility of deep out-of-money call minus the implied volatility of the deep out-of-money put. In this analysis we have used risk reversals constructed from 25-delta options of 1 month and 1 year maturity.

Table 2: **Serial dependence and greater extremes in yen *appreciation* jumps.** The table shows summary statistics for realized volatility jumps in JPY/USD exchange rate.

	Yen Appreciation Jumps			Yen Depreciation Jumps		
	κ_-	$\kappa_-(\alpha = 0.05)$	$\kappa_-(\alpha = 0.01)$	κ_+	$\kappa_+(\alpha = 0.05)$	$\kappa_+(\alpha = 0.01)$
Prop.	0.474	0.246	0.172	0.485	0.239	0.167
Obs.	1255	650	455	1276	628	438
Mean	0.044	0.026	0.019	0.036	0.022	0.016
St. Dev.	0.113	0.097	0.073	0.079	0.068	0.055
Skew.	10.543	14.290	8.575	6.521	8.803	7.876
Kurt.	202.355	351.193	110.709	77.961	133.712	105.325
Min.	0.000	0.000	0.002	0.000	0.000	0.001
Max.	2.959	2.959	1.386	1.482	1.482	1.125
Q-stat	161.899***	79.366***	133.528***	38.296***	33.733***	3.828

Notes: All jumps and jumps with $\alpha = 0.05$ and $\alpha = 0.01$. The Ljung-Box Q-test statistic (Q-stat) #lags=log(sample size); *,**, and *** indicate rejection of H_0 of white noise at 5%, 1% and 0.1% level of significance respectively. 01/01/1999 through 02/01/2007 sample period.

Table 3: **Subsample summary statistics for realized volatility jumps in JPY/USD exchange rate.**Samples split at $(i^{U.S.} - i^{JP}) = 2\%$ and VIX = 20 pts. Under a more conservative criteria only jumps significant at $\alpha = 0.01$ included.

	High Differential		Low Differential		High VIX		Low VIX	
	κ_-	κ_+	κ_-	κ_+	κ_-	κ_+	κ_-	κ_+
Prop.	10.51%	10.90%	6.69%	8.12%	9.34%	5.80%	7.83%	8.58%
Obs.	278	286	177	213	247	152	207	225
Mean	0.124	0.093	0.093	0.109	0.140	0.099	0.078	0.082
St. Dev.	0.160	0.089	0.113	0.098	0.177	0.126	0.080	0.107
Skew.	3.941	2.976	5.172	2.906	3.769	5.074	2.672	5.765
Kurt.	23.883	17.218	42.683	15.898	20.888	35.761	11.442	48.260
Min.	0.002	0.001	0.002	0.001	0.002	0.003	0.002	0.007
Max.	1.386	0.780	1.124	0.780	1.386	1.125	0.510	1.125
Q-stat	88.506***	1.399	46.481***	1.253	63.216***	4.708	25.4126***	3.616

Notes: Jumps with α=0.01. The Ljung-Box Q-test statistic (Q-stat) #lags=log(sample size); *,**, and *** indicate rejection of of white noise at 5%, 1% and 0.1% level of significance respectively. 01/01/1999 through 02/01/2007 sample period.

Table 4: **Non-linear dependence in realized volatility jumps** . The table show BDS test results, only yen *appreciation* jumps exhibit non-linear dependence.

	Yen Appreciation Jumps						Yen Depreciation Jumps					
	κ_-		$\kappa_-(\alpha = 0.05)$		$\kappa_-(\alpha = 0.01)$		κ_+		$\kappa_+(\alpha = 0.05)$		$\kappa_+(\alpha = 0.01)$	
dim.	BDS-stat	prob	BDS-stat	prob	BDS-stat	prob	BDS-stat	prob	BDS-stat	prob	BDS-stat	prob
2	0.024***	0.000	0.015***	0.000	0.008**	0.016	0.009***	0.000	0.002	0.554	0.005	0.144
	(0.003)		(0.003)		(0.003)		(0.003)		(0.003)		(0.004)	
3	0.043***	0.000	0.025***	0.000	0.016***	0.008	0.017***	0.000	0.002	0.698	0.007	0.222
	(0.004)		(0.005)		(0.006)		(0.004)		(0.005)		(0.006)	
4	0.055***	0.000	0.028***	0.000	0.022***	0.002	0.019***	0.000	0.001	0.850	0.007	0.278
	(0.005)		(0.006)		(0.007)		(0.005)		(0.006)		(0.007)	
5	0.063***	0.000	0.029***	0.000	0.022***	0.006	0.020***	0.000	0.002	0.730	0.007	0.300
	(0.005)		(0.006)		(0.007)		(0.005)		(0.006)		(0.007)	
6	0.065***	0.000	0.027***	0.000	0.020***	0.010	0.021***	0.000	0.002	0.622	0.004	0.490
	(0.005)		(0.006)		(0.007)		(0.005)		(0.006)		(0.007)	

Notes: Standard erros in parenthesis; *,**, and *** indicate rejection of the null of I.I.D. at 5%, 1% and 0.1% level of significance respectively Test parametrized to be most parsimonious to unknown distribution in the data so acceptance parameter selected such that 0.7 of the total number of pairs of points in the sample lie within the acceptance radius and p-values calculated by bootstrapping based on 1,000 repetitions. Embeding dimention (m) chosed as log(sample size) of the data.

Table 5: **Distribution parameter estimates for yen *appreciation* jumps.**Test the goodness of fit of exponentially dampened power-law $Pr(\kappa) \propto \kappa^{-\zeta} e^{-\phi\kappa}$ (an outcome of dependent events) versus Pareto (pure power-law) and log-normal (an outcome of independent events).

	κ_-			$\kappa_-(\alpha = 0.05)$			$\kappa_-(\alpha = 0.01)$		
Distribution	Power-Exp	Pareto	Log-N	Power-Exp	Pareto	Log-N	Power-Exp	Pareto	Log-N
Parameter 1	ζ	ζ	μ	ζ	ζ	μ	ζ	ζ	μ
	3.110	3.183	-0.776	2.377	2.615	-1.618	2.246	2.704	-1.501
	(0.193)	(0.258)	(0.056)	(0.199)	(0.207)	(0.041)	(0.204)	(0.223)	(0.048)
Parameter 2	ϕ		σ	ϕ		σ	ϕ		σ
	0.080		0.463	0.528		0.564	1.040		0.528
	(0.021)		(0.040)	(0.018)		(0.029)	(0.023)		(0.034)
Log Likelihood	39.012	38.993	9.387	209.283	208.458	146.591	128.253	127.160	89.240
AIC	-74.024	-75.986	-14.774	-414.566	-414.916	-289.182	-252.506	-252.320	-174.480
AICc	-73.845	-75.898	-14.595	-414.502	-414.884	-289.118	-252.406	-252.270	-174.380
Cutoff	0.291			0.107			0.124		
	(0.051)			(0.033)			(0.027)		
Tail Observations	70			190			123		
	(141.455)			(57.801)			(40.092)		
Total Observations	1,255			650			455		

Notes: The power exponent estimated via the maximum likelihood then select the minimum cutoff κ that gives the minimum KS-statistic. Standard errors in parentheses. Standard errors for ζ and ϕ calculated using Bayesian MCMC method based on 10,000 simulations.

Table 6: **Distribution parameter estimates for yen *depreciation* jumps.**Test the goodness of fit of exponentially dampened power-law $Pr(\kappa) \propto \kappa^{-\zeta} e^{-\phi\kappa}$ (an outcome of dependent events) versus Pareto (pure power-law) and log-normal (an outcome of independent events).

	κ_+			$\kappa_+(\alpha = 0.05)$			$\kappa_+(\alpha = 0.01)$		
Distribution	Power-Exp	Pareto	Log-N	Power-Exp	Pareto	Log-N	Power-Exp	Pareto	Log-N
Parameter 1	ζ	ζ	μ	ζ	ζ	μ	ζ	ζ	μ
	2.510	2.967	-1.502	2.928	3.065	-1.538	2.983	3.229	-1.547
	(0.202)	(0.224)	(0.036)	(0.203)	(0.286)	(0.045)	(0.203)	(0.395)	(0.047)
Parameter 2	ϕ		σ	ϕ		σ	ϕ		σ
	1.125		0.466	0.321		0.475	0.642		0.435
	(0.018)		(0.026)	(0.026)		(0.032)	(0.032)		(0.034)
Log Likelihood	198.864	197.884	142.702	145.335	145.234	99.382	117.424	117.284	84.037
AIC	-393.728	-393.768	-281.404	-286.670	-288.468	-194.764	-230.848	-232.568	-164.074
AICc	-393.549	-393.680	-281.225	-286.606	-288.436	-194.700	-230.748	-232.518	-163.974
Cutoff	0.134			0.132			0.136		
	(0.030)			(0.034)			(0.035)		
Tail Observations	168			115			87		
	(111.917)			(74.413)			(64.540)		
Total Observations	1,276			628			438		

Notes: The power exponent estimated via the maximum likelihood then select the minimum cutoff κ that gives the minimum KS-statistic. Standard errors in parentheses. Standard errors for ζ and ϕ calculated using Bayesian MCMC method based on 10,000 simulations.

Table 7: **Model distribution parameter estimates with alternative cut-off for the tail.**Exponentially dampened power-law $Pr(\kappa) \propto \kappa^{-\zeta} e^{-\phi\kappa}$ parameters estimated in the tail with cutoff at 1 standard deviation.

	κ_-	$\kappa_-(\alpha = 0.05)$	$\kappa_-(\alpha = 0.01)$	κ_+	$\kappa_+(\alpha = 0.05)$	$\kappa_+(\alpha = 0.01)$
ζ	2.288	2.230	1.527	2.146	2.049	1.495
	(0.197)	(0.196)	(0.201)	(0.200)	(0.200)	(0.201)
ϕ	0.713	0.744	2.480	1.858	1.992	4.324
	(0.026)	(0.035)	(0.041)	(0.028)	(0.039)	(0.046)
Cutoff	0.113	0.097	0.073	0.079	0.068	0.055
Log Likelihood	286.250	237.038	244.226	538.233	428.577	421.284
Tail Observations	274	211	210	368	283	268
Total Observations	1255	650	455	1276	628	438

Notes: Exponentially dampened power-law parameters re-estimated expanding cutoff for the tails of the distribution to 1 standard deviation bounds. Under this more inclusive specification a power law exponent of 1.5 is observed in the data. Standard errors in parentheses.

Table 8: **Distribution parameter estimates, sample split by interest rate differential.**Exponentially dampened power-law: $Pr(\kappa) \propto \kappa^{-\zeta} e^{-\phi\kappa}$. parameters estimated for samples split at $(i^{U.S.} - i^{JP}) = 2\%$

	High Interest Rate Differential						Low Interest Rate Differential					
	$\kappa_-(\alpha = 0.01)$			$\kappa_+(\alpha = 0.01)$			$\kappa_-(\alpha = 0.01)$			$\kappa_+(\alpha = 0.01)$		
Distribution	Power-Exp	Pareto	Log-N	Power-Exp	Pareto	Log-N	Power-Exp	Pareto	Log-N	Power-Exp	Pareto	Log-N
Parameter 1	ζ	ζ	μ	ζ	ζ	μ	ζ	ζ	μ	ζ	ζ	μ
	2.007	2.569	-1.530	2.769	3.610	-1.461	2.394	2.874	-1.785	2.894	2.932	-1.745
	(0.194)	(0.406)	(0.057)	(0.200)	(0.690)	(0.052)	(0.204)	(0.511)	(0.065)	(0.198)	(0.439)	(0.081)
Parameter 2	ϕ		σ	ϕ		σ	ϕ		σ			σ
	1.250		0.561	2.408		0.355	1.410		0.487	0.094		0.531
	(0.060)		(0.041)	(0.100)		(0.038)	(0.106)		(0.047)	(0.114)		(0.059)
Log Likelihood	92.538	93.749	65.281	68.830	68.576	51.153	78.550	81.079	61.272	63.659	63.671	42.640
AIC	-173.555	-174.645	-107.208	-150.100	-151.519	-110.284	-281.040	-286.469	-230.115	-87.736	-95.227	-57.988
AICc	-173.417	-174.577	-107.070	-149.860	-151.401	-110.044	-280.896	-286.398	-229.970	-87.372	-95.051	-57.624
Cutoff	0.1138			0.1568			0.0975			0.1029		
	(0.063)			(0.049)			(0.031)			(0.024)		
Tail Observations	94		.	48			56			44		
	(46.707)			(55.433)			(32.467)			(21.661)		
Total Observations	278			286			177			152		

Notes: The power exponent estimated via the maximum likelihood then select the minimum cutoff κ that gives the minimum KS-statistic. Standard errors in parentheses. Standard errors for ζ and ϕ calculated using Bayesian MCMC method based on 10,000 simulations. Sample split into jumps associated with the interest rate differential above and below 2%.

Table 9: **Distribution parameter estimates, subsample split by VIX.**Exponentially dampened power-law $Pr(\kappa) \propto \kappa^{-\zeta} e^{-\phi\kappa}$ parameters estimated for samples split at VIX = 20 pts.

	High VIX						Low VIX					
	$\kappa_-(\alpha = 0.01)$			$\kappa_+(\alpha = 0.01)$			$\kappa_-(\alpha = 0.01)$			$\kappa_+(\alpha = 0.01)$		
Distribution	Power-Exp	Pareto	Log-N	Power-Exp	Pareto	Log-N	Power-Exp	Pareto	Log-N	Power-Exp	Pareto	Log-N
Parameter 1	ζ	ζ	μ	ζ	ζ	μ	ζ	ζ	μ	ζ	ζ	μ
	2.358	2.664	-1.466	2.719	3.398	-1.539	1.933	2.682	-2.131	2.885	3.035	-1.590
	(0.190)	(0.212)	(0.059)	(0.198)	(0.558)	(0.053)	(0.198)	(0.324)	(0.056)	(0.196)	(0.333)	(0.086)
Parameter 2	ϕ		σ	ϕ		σ	ϕ		σ	ϕ		σ
	0.620		0.564	1.999		0.387	3.327		0.526	0.223		0.509
	(0.060)		(0.043)	(0.098)		(0.039)	(0.099)		(0.040)	(0.120)		(0.063)
Log Likelihood	88.777	88.323	55.604	77.050	76.759	57.142	142.520	144.235	117.057	45.868	48.614	30.994
AIC	-173.555	-174.645	-107.208	-150.100	-151.519	-110.284	-281.040	-286.469	-230.115	-87.736	-95.227	-57.988
AICc	-173.417	-174.577	-107.070	-149.860	-151.401	-110.044	-280.896	-286.398	-229.970	-87.372	-95.051	-57.624
Cutoff	0.1257			0.1403			0.0651			0.1231		
	(0.019)			(0.037)			(0.019)			(0.025)		
Tail Observations	90			53			86			36		
	(17.934)			(36.537)			(23.712)			(34.358)		
Total Observations	248			213			207			225		

Notes: The power exponent estimated via the maximum likelihood then select the minimum cutoff κ that gives the minimum KS-statistic. Standard errors in parentheses. Standrad errors for ζ and ϕ calculated using Bayesian MCMC method based on 10,000 simulations. Sample split into jumps associated with the VIX above and below 20 points.

Table 10: **Economic determinants of "tail risk" of yen appreciation.**Higher ϕ corresponds to faster exponential truncation in the tail of the probability distribution; ϕ is inversely related to the "tail risk".

Variable	Impact on ϕ	Description	Proxy
k	-	Cumulative carry position	CME non-commercial yen short futures positions Sample: 01/01/1999-02/01/2007 Source: CFTC
$(\Delta s_H - \Delta s_L)$	-	Expected dollar devaluation	Value of 10 delta 1-year yen-dollar risk reversal Sample: 09/28/2003-02/01/2007 Source: Bloomberg
M	+	Margin requirement	Initial speculator margin for yen futures on CME Sample: 01/01/1999-02/01/2007 Source: CME Group
ρ	-	Risk aversion	CBOE S&P 500 options implied volatility index (VIX) Sample: 01/01/1999-02/01/2007 Source: WRDS

Notes: Although risk aversion (ρ) is not modeled explicitly, we control for it with VIX. We do this for two reasons: first, to the extent that VIX proxies not only for risk aversion but also for funding conditions it is an important variable for gaging speculative forces in foreign exchange and second, since the value of risk reversals conveys option implied skewness *and* skewness risk premium, or equivalently $(\Delta s_H - \Delta s_L)\rho$, it is necessary to control for risk aversion with a proxy such as the VIX.

Table 11: **Impact of carry trade factors on the "tail risk".**Higher ϕ corresponds to faster exponential truncation in the tail of the probability distribution; ϕ is inversely related to the "tail risk".

	Dependent parameter: the speed of probability decline in the tail (ϕ)					
	(1)	(2)	(3)	(4)	(5)	(6)
Non-Commercial Shorts (k)	-1.201**		-1.220**	-1.912**	-1.945***	
	(0.542)		(0.592)	(0.739)	(0.734)	
Monte Carlo S.E.	0.016		0.020	0.028	0.025	
VIX (ρ)		-1.838***	-0.326	-1.292	-1.228	
		(0.581)	(0.985)	(1.004)	(0.966)	
Monte Carlo S.E.		0.026	0.031	0.028	0.024	
CME Margin Requirement (M)				1.019	1.024	
				(0.729)	(0.719)	
Monte Carlo S.E.				0.026	0.023	
Risk Reversals ($\Delta s_H - \Delta s_L$)					-0.685	-1.451**
					(0.944)	(0.711)
Monte Carlo S.E.					0.026	0.024
τ_ϵ	0.727	0.743	0.542	0.604	0.592	0.800
	(0.559)	(0.601)	(0.436)	(0.540)	(0.529)	(0.575)
Monte Carlo S.E.	0.050	0.053	0.037	0.048	0.036	0.030
Observations	123	123	123	123	24	24

Notes: Results based on 10,000 samples after discarding the first 4,000 iterations as "burn-in". Standard errors in parenthesis. *, **, and *** indicate coefficients significant at 10%, 5%, and 1% level respectively under the normality assumption for the simulated parameter values.

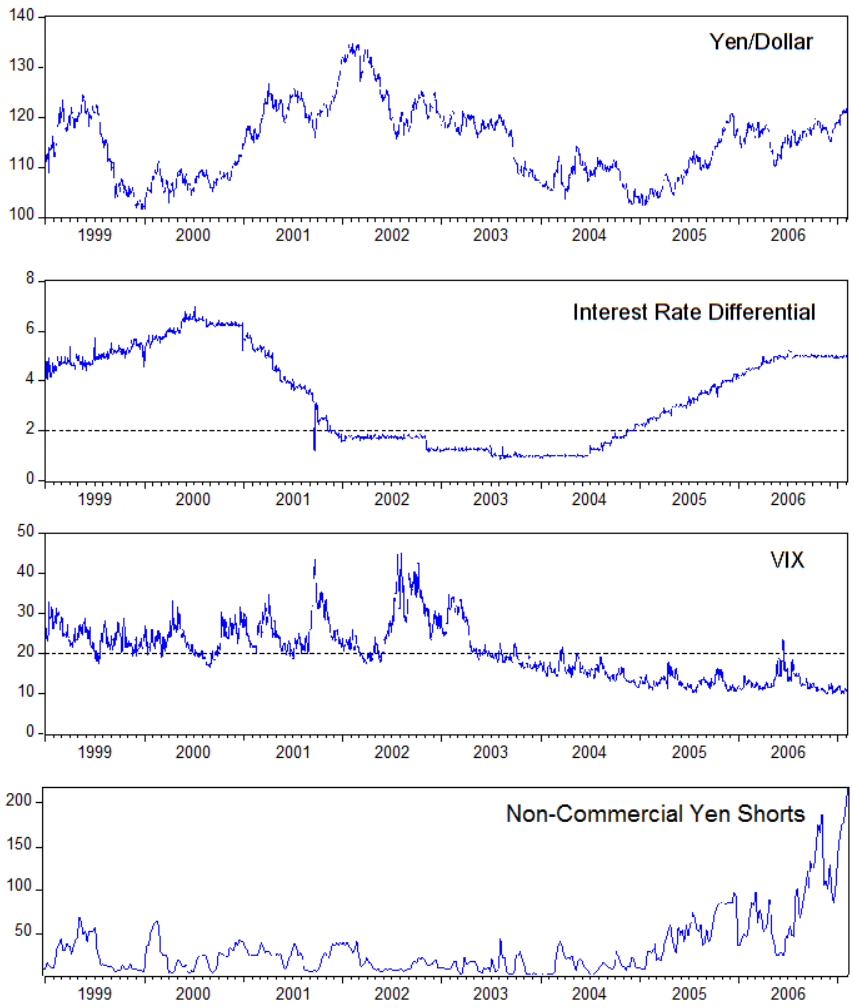

Figure 1: **Main time series.**Daily time series of JPY/USD exchange rate, U.S.-Japan interest rate differential, CBOE VIX, and Non-commercial short futures positions in Yen (thousands of contract units); 01/01/1999 through 02/01/2007 sample period. In strong violation of the UIP an increase in the interest rate spread corresponded with dollar appreciation against the yen. Combined, these trends suggest that carry trade may have been a major factor in JPY/USD exchange rate dynamic during our sample period.

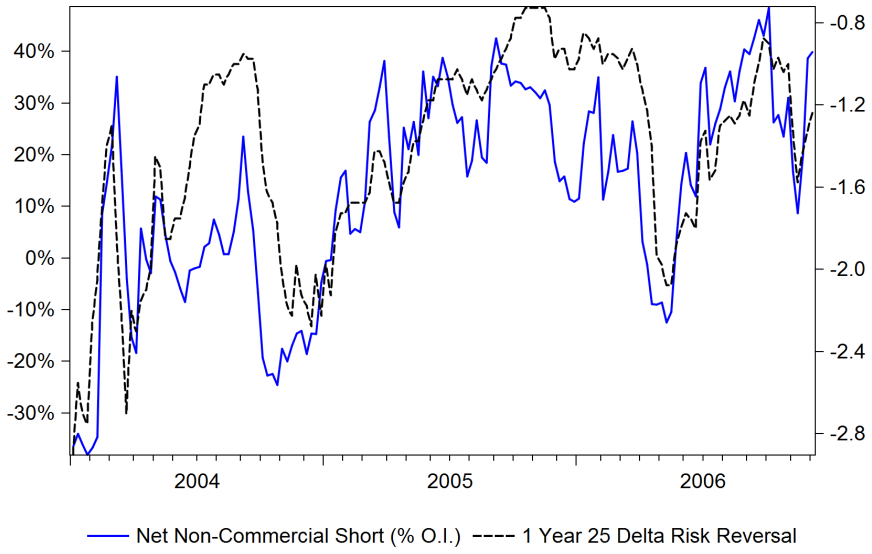

Figure 2: **Speculative futures positions in yen and the cost of hedging against large yen appreciation.**The negative values of risk reversals indicates a market hedge against sharp yen appreciation during the height of yen carry trade (the entire 2004-2006 period). The close association between risk reversals and net speculative short positions in yen indicates that risk reversals contain important information to carry traders on the currency risk of their positions and corroborating the notion that "day of reckoning" considerations are central to carry trade.

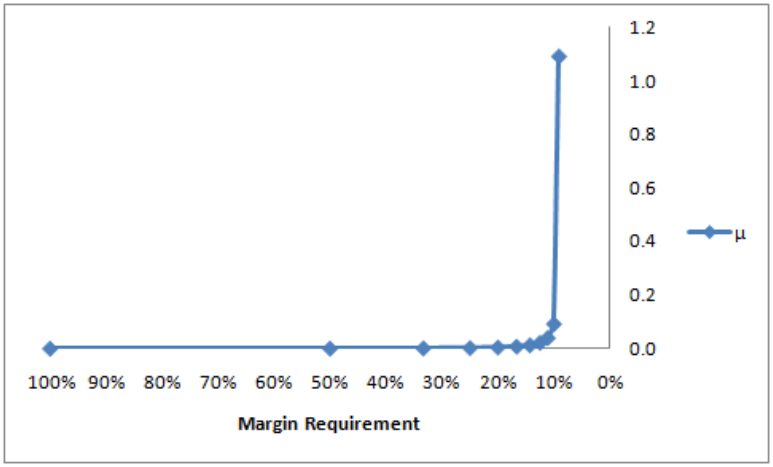

Figure 3: **Margin requirement and herding.**When margin requirement is high then a reduction in margin requirement has virtually no effect on the intensity of the branching process measured by μ (herding). However, when the margin requirement is lowered below a certain threshold (approximately 20%), then the branching process begins to intensify exponentially. When the margin requirement reaches second threshold (approximately 10%) then μ is suddenly taken from subcritical ($\mu < 1$) to superctitical state ($\mu > 1$), implying an "explosive" episode of carry trader unwinding. Set $\Delta s_H = 0.05$, $\Delta s_L = -0.07$, $\delta = 0.04$, and $k = 100,000$.

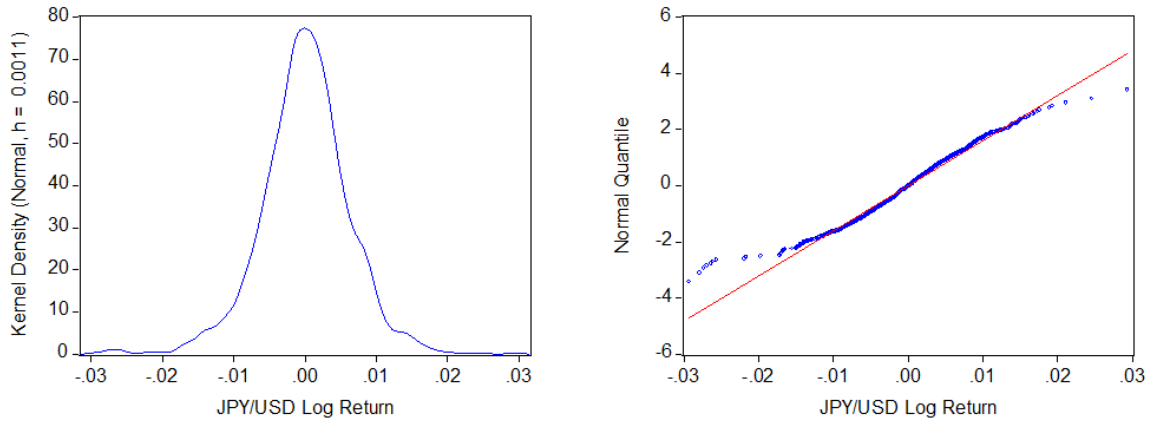

Figure 4: **Distribution of JPY/USD Log Returns.** *Left:* Kernel density; *Right:* Q-Q plot versus normal distribution. The leptokurtic features are apparent, with a fatter negative tail (yen appreciations) which also exhibits larger deviation from the normal hypothesis.

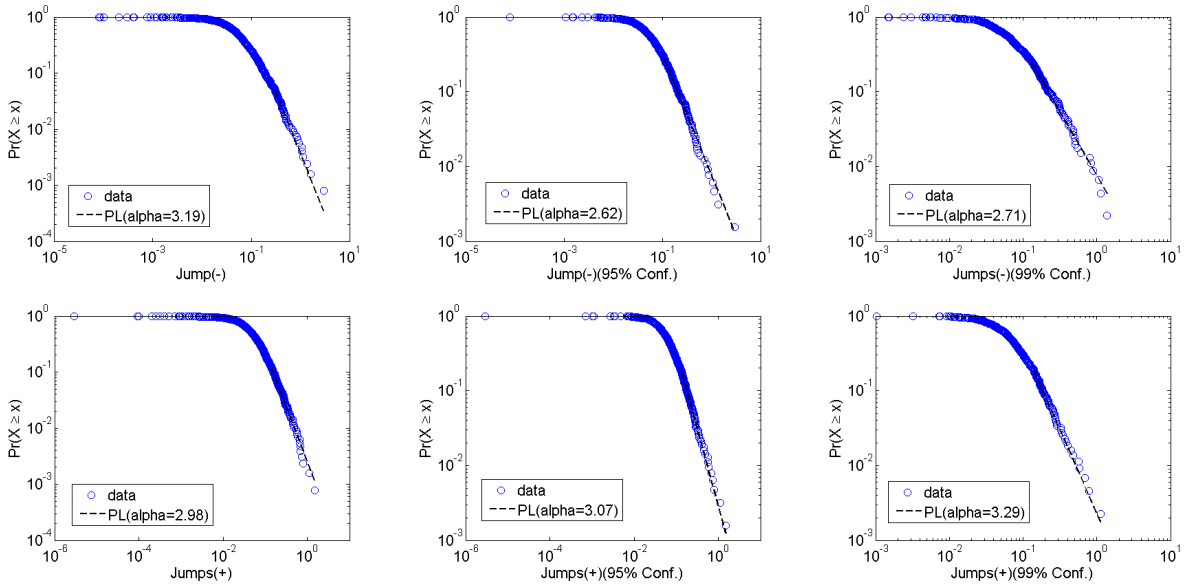

Figure 5: **Power-law in the tail distribution of JPY/USD returns.** *Top:* Yen appreciation jumps; *Bottom:* Yen depreciation jumps. The probability plots for positive and negative jumps for each level of significance on a log-log scale. The fitted straight line on the log-log probability plot indicates that distributions of jumps exhibit strong power-law tails.

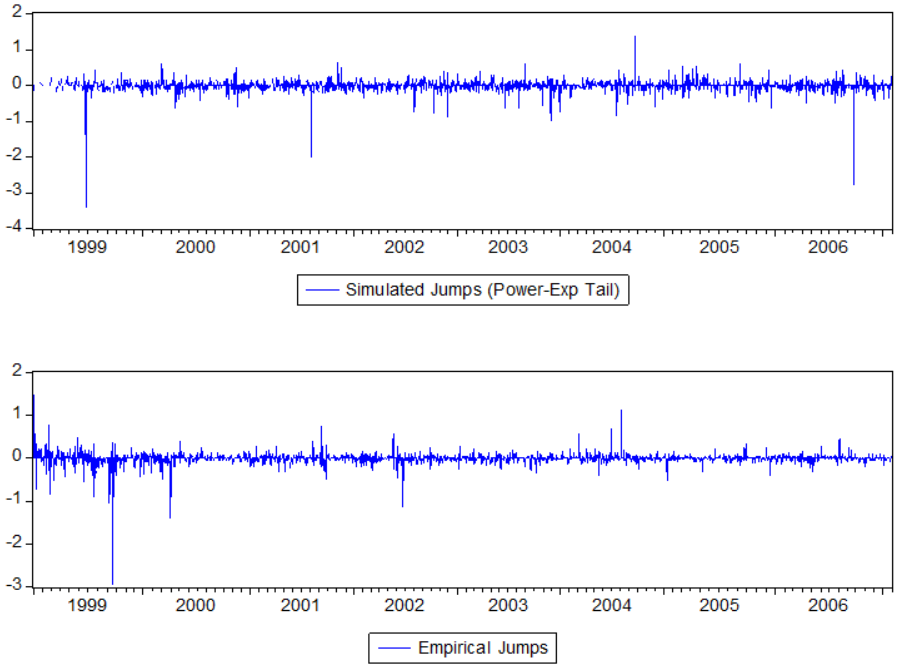

Figure 6: **Simulation based on exponentially dampened power-law.** *Top:* Jumps in JPY/USD simulated using exponentially dampened power-law with parameters cutoff=0.124, ζ=2.246, ϕ=1.040 for κ_- and cutoff=0.136, ζ=2.983, ϕ=0.642 for κ_+; *Bottom:* Empirical realized volatility jumps series. The simulation results indicate that the underlying data generating process is different for negative and positive jumps, with negative jumps subject to more extreme fluctuations. The contrast between simulation of yen appreciation (negative) and yen depreciation (positive) jumps captures the negative skewness of JPY/USD returns.

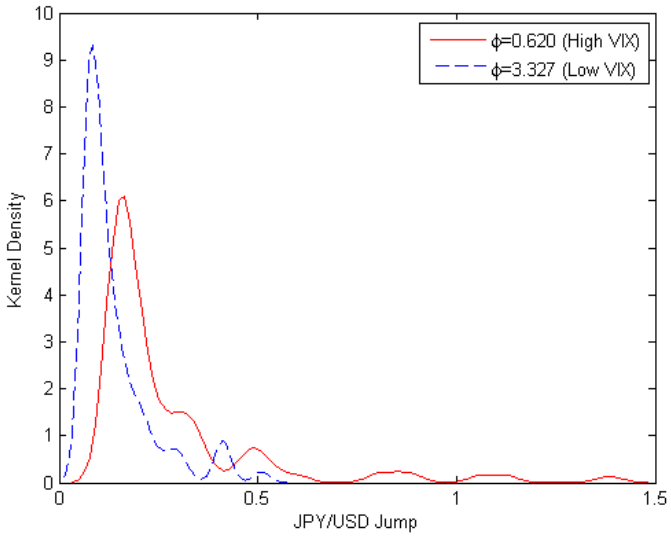

Figure 7: **VIX and the "tail risk" of sharp yen appreciation.**The figure shows kernel density plots of yen *appreciation* jumps for subsamples for high and low VIX (cutoff at 20 points). Lower ϕ during high VIX periods indicates a more stretched tail of the distribution corresponding to higher risk of sharp yen appreciation.

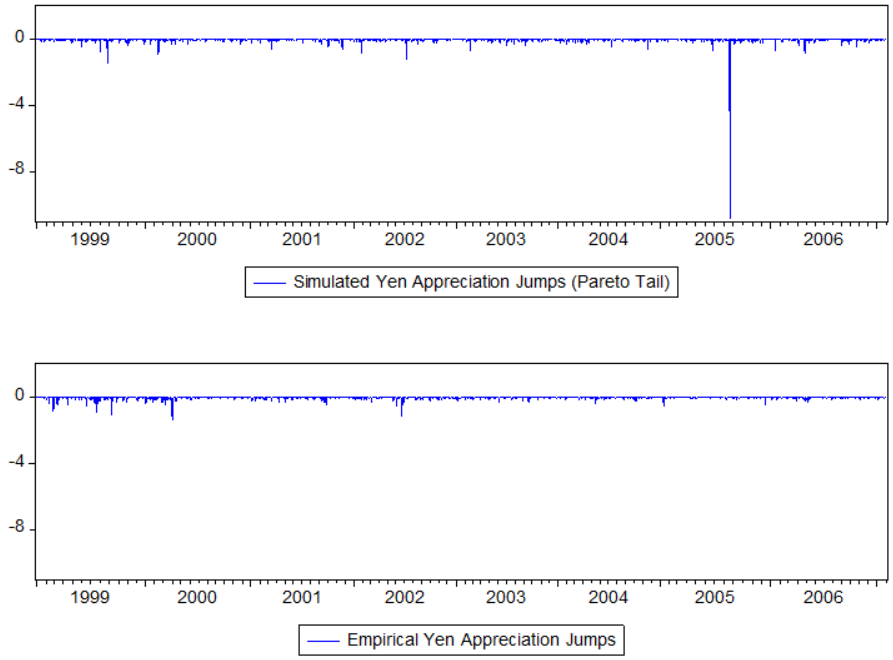

Figure 8: **Simulation based on extreme case of $\phi = 0$ (pure power-law).** *Top:* Jumps in JPY/USD simulated using pure power-law with parameters cutoff=0.124, ζ=2.704; *Bottom:* empirical realized volatility jump series. The simulation approximates the general amplitude in the fluctuations of the empirical data shown in the bottom panel except for the one "catastrophic" event when the simulated jump exceeds 11 in absolute value exposing the "hidden tail risk".

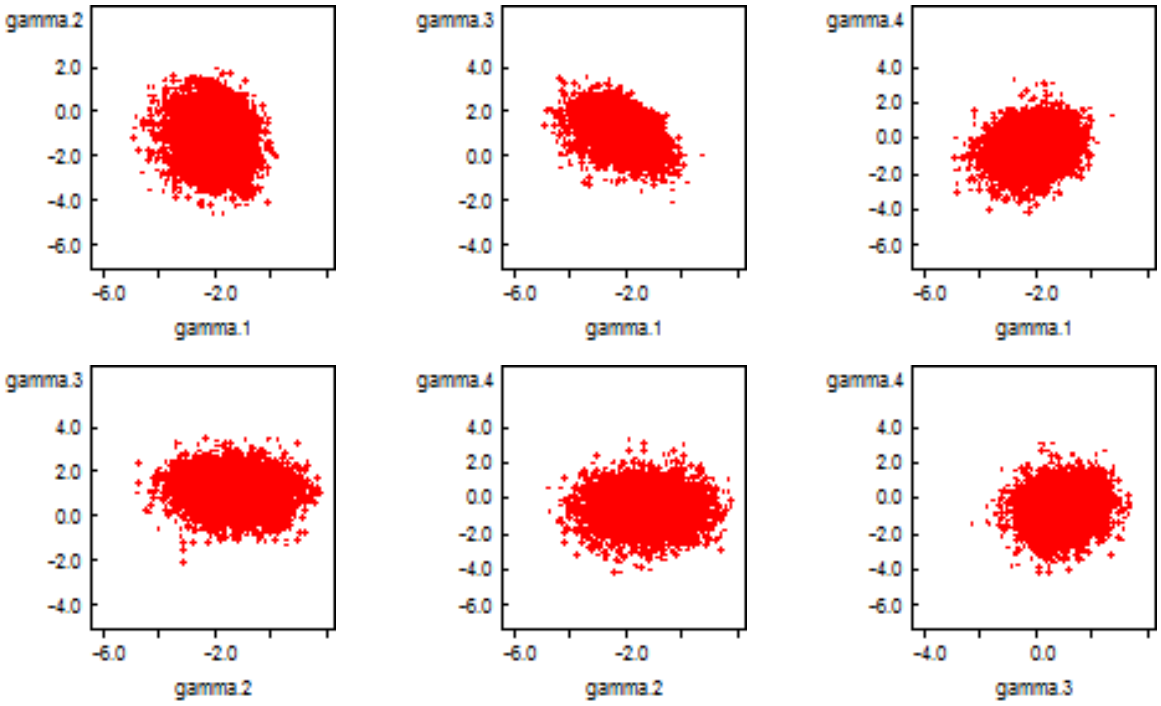

Figure 9: **Scatter plot of sampled coefficients.** γ_1, γ_2, γ_3, and γ_4 are coefficients on CME speculative positions, VIX, CME margin requirement, and risk reversals respectively in specification (5) of impact of carry trade factors on the speed of probability decline in the tail (ϕ). While most scatter plots show a random spread (no multicollinearity) the scatter plot between γ_1 and γ_3 (γ_1 and γ_4) exhibit a negative (positive) correlation.

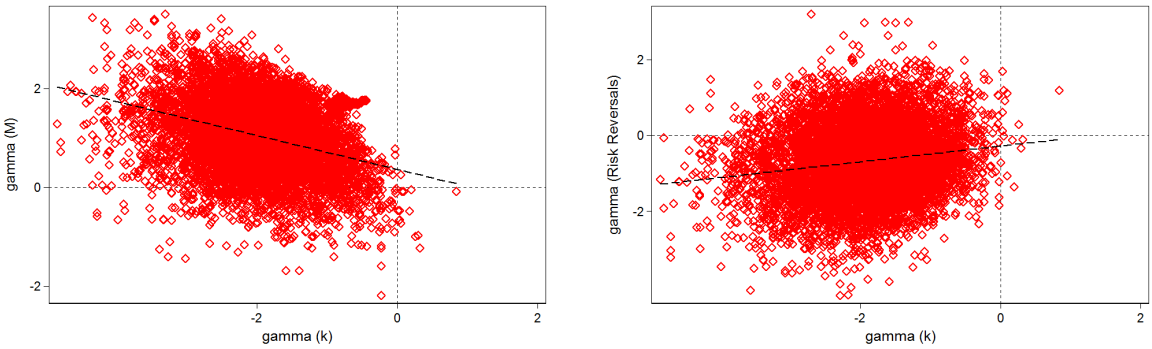

Figure 10: **The blowup of selected scatter plots.** *Left:* coefficients on speculative positions and margin requirement *Right:* coefficients on speculative positions and risk reversals; in specification (5) of impact of carry trade factors on the speed of probability decline in the tail (ϕ). The correlation between coefficients on speculative positions and margin requirement (γ_1 and γ_3) is -0.3528 and the correlation between coefficients on speculative positions and risk reversals (γ_1 and γ_4) is 0.1650, with $p-value$=0.0000 for both. This indicates that tougher margin requirements have an effect of reducing probability of extreme yen appreciation by mitigating the impact of carry trade activity, and, similarly, expectations of sharp yen appreciation tend to be self-fulfilling and further increase the probability of extreme yen appreciation through the actions of carry traders.

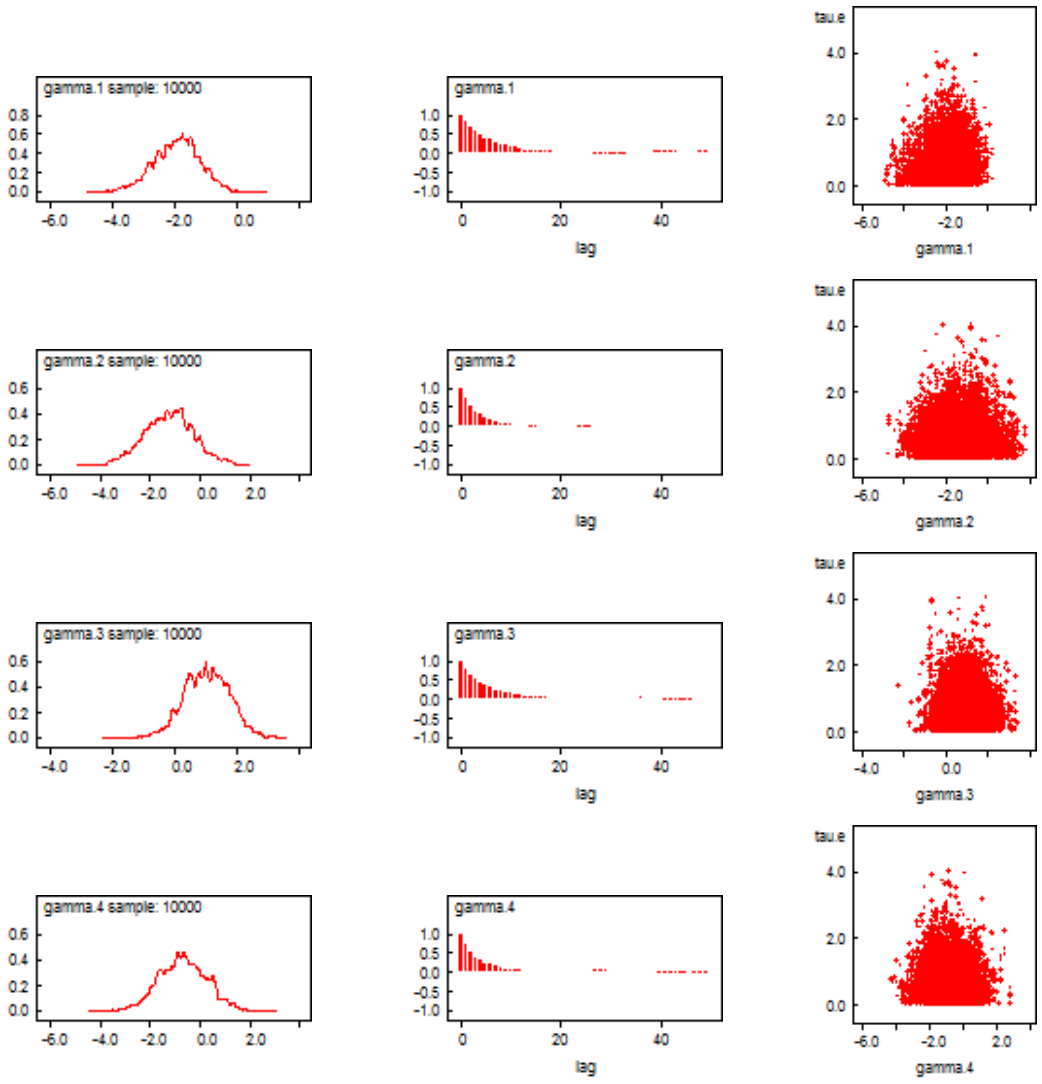

Figure 11: **Bayesian MCMC diagnostic plots for coefficients on speculative positions, VIX, margin requirement, and risk reversals in the specification (5) of impact of carry trade factors on the speed of probability decline in the tail (ϕ).** *Left:* density of the samples with a bell curve indicating a good mixture and that a normal approximation to the standard errors is reasonable. *Center:* the rapidly declining autocorrelation function of the samples indicating a rapid mixing with estimates theselves approaching white noise. *Right:* a visual test for endogeneity via a scatter plot between sampled slope coefficient and random effects component, τ_ϵ, which is bounded at zero from below. The scatter plots show a random spread consistent with exogeneity of the controls.

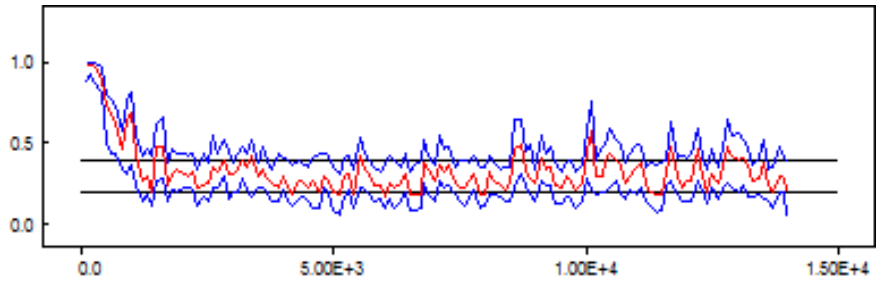

Figure 12: **Metropolis acceptance rates for specification (5) of impact of carry trade factors on the speed of probability decline in the tail (ϕ).**Acceptance rates reaching the stationary level around the commonly accepted level of 0.234 for random walk Metropolis-Hastings algorithm within 1,000 to 2,000 samples; we discard the first 4,000 using the subsequent 10,000 for inference.

Japanese Yen (JY) Performance Bond History
Minimum Performance Bond Requirements
Futures Opening Day: 5/16/1972
Options Opening Day: 3/5/1986

	Initial	Maint
8/17/2007		
Spec	$2,700	$2,000
Hedge/Member	$2,000	$2,000
7/31/2007		
Spec	$2,025	$1,500
Hedge/Member	$1,500	$1,500
6/11/2007		
Spec	$2,430	$1,800
Hedge/Member	$1,800	$1,800
3/1/2007		
Spec	$2,700	$2,000
Hedge/Member	$2,000	$2,000
1/25/2007		
Spec	$2,160	$1,600
Hedge/Member	$1,600	$1,600
10/17/2006		
Spec	$2,430	$1,800
Hedge/Member	$1,800	$1,800
3/15/2006		
Spec	$2,700	$2,000
Hedge/Member	$2,000	$2,000
2/6/2006		
Spec	$3,105	$2,300
Hedge/Member	$2,300	$2,300
12/15/2005		
Spec	$3,510	$2,600
Hedge/Member	$2,600	$2,600
12/8/2005		
Spec	$2,025	$1,500
Hedge/Member	$1,500	$1,500
11/2/2005		
Spec	$2,295	$1,700
Hedge/Member	$1,700	$1,700
7/26/2005		
Spec	$2,700	$2,000
Hedge/Member	$2,000	$2,000
4/28/2005		
Spec	$2,160	$1,600
Hedge/Member	$1,600	$1,600
4/1/2005		
Spec	$2,363	$1,750
Hedge/Member	$1,750	$1,750
1/14/2005		
Spec	$2,565	$1,900
Hedge/Member	$1,900	$1,900
12/27/2004		
Spec	$2,228	$1,650
Hedge/Member	$1,650	$1,650
9/28/2004		
Spec	$2,430	$1,800
Hedge/Member	$1,800	$1,800
9/1/2004		
Spec	$2,700	$2,000
Hedge/Member	$2,000	$2,000
7/30/2004		
Spec	$2,835	$2,100
Hedge/Member	$2,100	$2,100
5/27/2004		
Spec	$3,105	$2,300
Hedge/Member	$2,300	$2,300
3/25/2004		
Spec	$2,228	$1,650
Hedge/Member	$1,650	$1,650
10/2/2003		
Spec	$1,755	$1,300
Hedge/Member	$1,300	$1,300
7/7/2003		
Spec	$1,890	$1,400
Hedge/Member	$1,400	$1,400
3/6/2003		
Spec	$2,160	$1,600
Hedge/Member	$1,600	$1,600
12/5/2002		
Spec	$2,295	$1,700
Hedge/Member	$1,700	$1,700
5/30/2002		
Spec	$2,430	$1,800
Hedge/Member	$1,800	$1,800
4/9/2002		
Spec	$2,700	$2,000
Hedge/Member	$2,000	$2,000
3/12/2002		
Spec	$1,890	$1,400
Hedge/Member	$1,400	$1,400
8/1/2001		
Spec	$2,025	$1,500
Hedge/Member	$1,500	$1,500
5/3/2001		
Spec	$2,835	$2,100
Hedge/Member	$2,100	$2,100
3/1/2001		
Spec	$2,025	$1,500
Hedge/Member	$1,500	$1,500
2/1/2001		
Spec	$2,835	$2,100
Hedge/Member	$2,100	$2,100
1/4/2001		
Spec	$2,025	$1,500
Hedge/Member	$1,500	$1,500

738

Revised: 01/03/08

Figure 13: **Sample CME Margin Requirement Report**We use initial speculator ("Spec") margin requirement data to proxy for margin requirements faced by carry traders in Japanese yen. (Source: CME Group.)

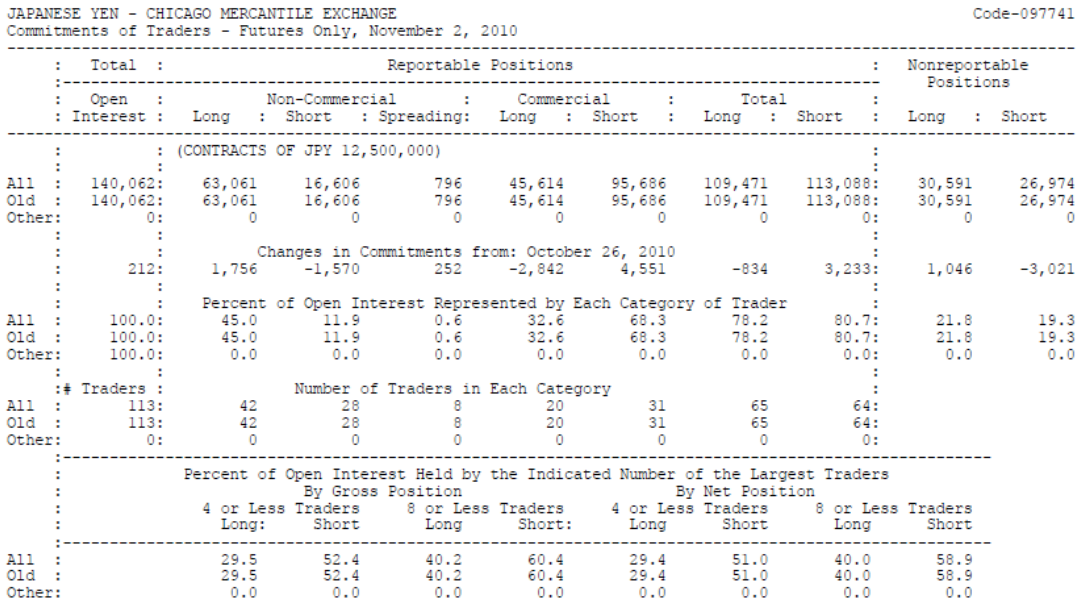

JAPANESE YEN - CHICAGO MERCANTILE EXCHANGE — Code-097741
Commitments of Traders - Futures Only, November 2, 2010

	Total	Reportable Positions							Nonreportable Positions	
	Open Interest	Non-Commercial Long	Non-Commercial Short	Non-Commercial Spreading	Commercial Long	Commercial Short	Total Long	Total Short	Long	Short
	(CONTRACTS OF JPY 12,500,000)									
All	140,062	63,061	16,606	796	45,614	95,686	109,471	113,088	30,591	26,974
Old	140,062	63,061	16,606	796	45,614	95,686	109,471	113,088	30,591	26,974
Other	0	0	0	0	0	0	0	0	0	0
	Changes in Commitments from: October 26, 2010									
	212	1,756	-1,570	252	-2,842	4,551	-834	3,233	1,046	-3,021
	Percent of Open Interest Represented by Each Category of Trader									
All	100.0	45.0	11.9	0.6	32.6	68.3	78.2	80.7	21.8	19.3
Old	100.0	45.0	11.9	0.6	32.6	68.3	78.2	80.7	21.8	19.3
Other	100.0	0.0	0.0	0.0	0.0	0.0	0.0	0.0	0.0	0.0
# Traders		Number of Traders in Each Category								
All	113	42	28	8	20	31	65	64		
Old	113	42	28	8	20	31	65	64		
Other	0	0	0	0	0	0	0	0		

	Percent of Open Interest Held by the Indicated Number of the Largest Traders							
	By Gross Position				By Net Position			
	4 or Less Traders Long	4 or Less Traders Short	8 or Less Traders Long	8 or Less Traders Short	4 or Less Traders Long	4 or Less Traders Short	8 or Less Traders Long	8 or Less Traders Short
All	29.5	52.4	40.2	60.4	29.4	51.0	40.0	58.9
Old	29.5	52.4	40.2	60.4	29.4	51.0	40.0	58.9
Other	0.0	0.0	0.0	0.0	0.0	0.0	0.0	0.0

Figure 14: **Sample CFTC Commitments of Traders Report**Following Klitgaard and Weir (2004), Galati, Heath and McGuire (2007), Brunnermeier et al. (2009) Cecchetti et al. (2010) and others we proxy for the changes in the volume of carry trade by changes in non-commercial yen short futures positions on The Chicago Mercantile Exchange. (Source: http://www.cftc.gov/MarketReports/CommitmentsofTraders/.)